# Microearthquakes, Swarms, and the Geothermal Areas of Iceland[1]

PETER L. WARD

*Lamont-Doherty Geological Observatory of Columbia University*
*Palisades, New York 10964*

SVEINBJÖRN BJÖRNSSON

*National Energy Authority, Reykjavík, Iceland*

More than 2100 microearthquakes were recorded and crudely located by using data from portable seismographs operated in Iceland during the summer of 1968. Another 600 events were located more precisely in three areas by using data from tripartite arrays. The earthquakes recorded are largely confined to 13 regions that are generally less than 100 km² in area. Most of the well-located events are at depths of 2 to 6 km but some less well located events may be as deep as 13 km. The microearthquakes are largely confined to the upper few kilometers of the oceanic layer, or layer 3 ($Vp \approx 6.5$ km/sec in Iceland). Geothermal areas in Iceland that are structurally related to a large number of faults and fissures generally have high microearthquake activity. Geothermal areas that have few fissures and appear to be structurally related to acidic intrusions contain little or no microearthquake activity. The distribution of zones of microearthquake activity generally supports the hypothesis of a transform fault in southern Iceland. It appears that the stress along this fault is being relieved in geothermal areas by numerous microearthquake swarms occurring more or less continuously. Outside the geothermal areas, mainshock-aftershock sequences seem to be the dominant mode of stress release. The swarms can be attributed to weakening of the crust by fluids or fluid pressure.

During the summers of 1967 and 1968, surveys of microearthquake activity were conducted for the first time and largely on a reconnaisance basis throughout a substantial part of Iceland. Results from the field program of 1967 are presented by *Ward et al.* [1969]. This paper presents information gathered in 1968 and an analysis of microearthquake phenomena during both years.

Microearthquakes discussed here are earthquakes as small as magnitude −1. Up to 100,000 microearthquakes might occur in an area where only one event of magnitude greater than or equal to 4 is located during the same time with data from the standard types of seismograph stations commonly used around the world. Hence, a great deal of information on an area can be obtained in a short time by operating sensitive instruments in the field near the earthquake epicenters. Microearthquakes are generally so small that in this study few events would have been recorded if instruments had not been placed within 30 km of the active zones.

In general, there is abundant microearthquake activity in Iceland; some 2700 events were recorded during two months in 1968, but the activity was confined largely to 13 zones, each with areas usually less than 100 km². Comparison with data for other regions of the world is difficult because of differences in recording conditions, hypocentral distances, instrumentation, etc., but the average level of microearthquake activity in Iceland seems to be higher but within an order of magnitude of that observed in Kenya [*Tobin et al.*, 1969], west-central Nevada [*Oliver et al.*, 1966], southern California [*Brune and Allen*, 1967], and Mt. Tsukuba, Japan [*Asada*, 1957].

It has been assumed until now that earthquakes in Iceland [*Stefánsson*, 1967] and along

[1] Lamont-Doherty Geological Observatory Contribution 1654.

the mid-Atlantic ridge are shallow, but there have been few data to show how shallow. More than 600 microearthquakes were reliably located in this study. They occurred primarily at depths of 2 to 6 km, a few being as deep as 13 km. The well-located microearthquakes occur primarily in the upper few kilometers of layer 3, or the oceanic layer [*Ewing and Ewing*, 1959] ($Vp \approx 6.5$ to 6.7 km/sec).

The spatial pattern of the zones of significant microearthquake activity in Iceland is an important source of information. On an island-wide scale, it appears to provide support for the spreading ridge–transform fault hypothesis discussed in detail by *Ward et al.* [1969] and *Ward* [1970].

Most of the microearthquakes recorded in Iceland are associated with major geothermal areas. A detailed study of two geothermal areas shows that the epicenters of the microearthquakes are nearly confined to the zone of thermal alteration observed at the surface. The most dense clusters often lie near the most intense zones of thermal activity. Microearthquakes have been observed in other geothermal areas such as the geysers in California [*Lange and Westphal*, 1969] and in Ahuachapan, El Salvador [*Ward and Jacob*, 1971]. This observation is of considerable practical significance, because it gives another method for studying geothermal processes and locating new geothermal areas. Nearly one-half the homes in Iceland are heated with natural hot water, and about 20% of the country's net energy consumption is based on natural heat resources [*Björnsson*, 1967]. A concerted effort was made to find a relationship between the operation of a large geothermal well and the temporal or spatial occurrence of microearthquakes, but none was discovered.

It is suggested that the stress along a transform fault in southern Iceland is relieved by quasi-continuous microearthquake swarms in the geothermal areas but by mainshock-aftershock earthquake sequences elsewhere in the fault zone. The crust in the geothermal areas may be weakened by the physical-chemical effects of fluids or by fluid pressure.

In the following sections, each of the principal points described above is discussed in some detail, and the supporting evidence is presented.

## Spatial Distribution of Microearthquakes throughout Iceland

During the summers of 1967 and 1968, high-gain portable seismographs were operated throughout Iceland at 154 sites, producing an average of 38 hours of clear, low-noise records at each site. The instruments and survey techniques are described by *Ward et al.* [1969]. Nearly all the microearthquakes recorded were in 13 zones, each with radii generally less than 5 km. The locations of these zones are shown in Figure 1, along with the major geothermal areas in Iceland, the zone of active rifting and volcanism or neovolcanic zone, and the distribution of large earthquakes from 1967 through 1969 reported by the U.S. Coast and Geodetic Survey. The amount of activity observed from the 13 zones and the numbers of events recorded at each site are dependent on the temporal stability of the microearthquake activity and the attenuation of seismic waves as a function of distance and as a function of special geologic conditions along the wave path. Therefore, before the relation of microearthquakes to regions of geothermal activity and fracture zones is discussed, the data will be summarized and the effects of the short length of sampling time and the influence of attenuation will be presented.

*Data collected with portable stations in 1968.* Five portable seismographs were operated individually at a total of 87 sites during July and August 1968. Nine of the sites had been occupied during 1967. All sites are shown in Figure 2, and the data recorded at each site are given in Table 1. Data for 1967 and 1968 are summarized in Figure 3. The numbers in Figure 3 are the average numbers of events per day with $S$–$P$ times $\leq 2.5$ sec, corresponding to distances less than about 20 km, and with maximum trace amplitude $\geq 2$ mm at 30-db attenuation from a maximum gain of about 26 million. Although this magnitude is poorly defined for microearthquakes, the 2-mm amplitude limit roughly corresponds to a magnitude of about $-0.7$ [*Ward et al.*, 1969] for events close to the station where *Brune and Allen's* [1967] amplitude-versus-distance correction for 20-cps seismic waves is assumed to be negligible.

The most important observation in Figure 3 is that even though the recording stations were spread throughout most of Iceland, micro-

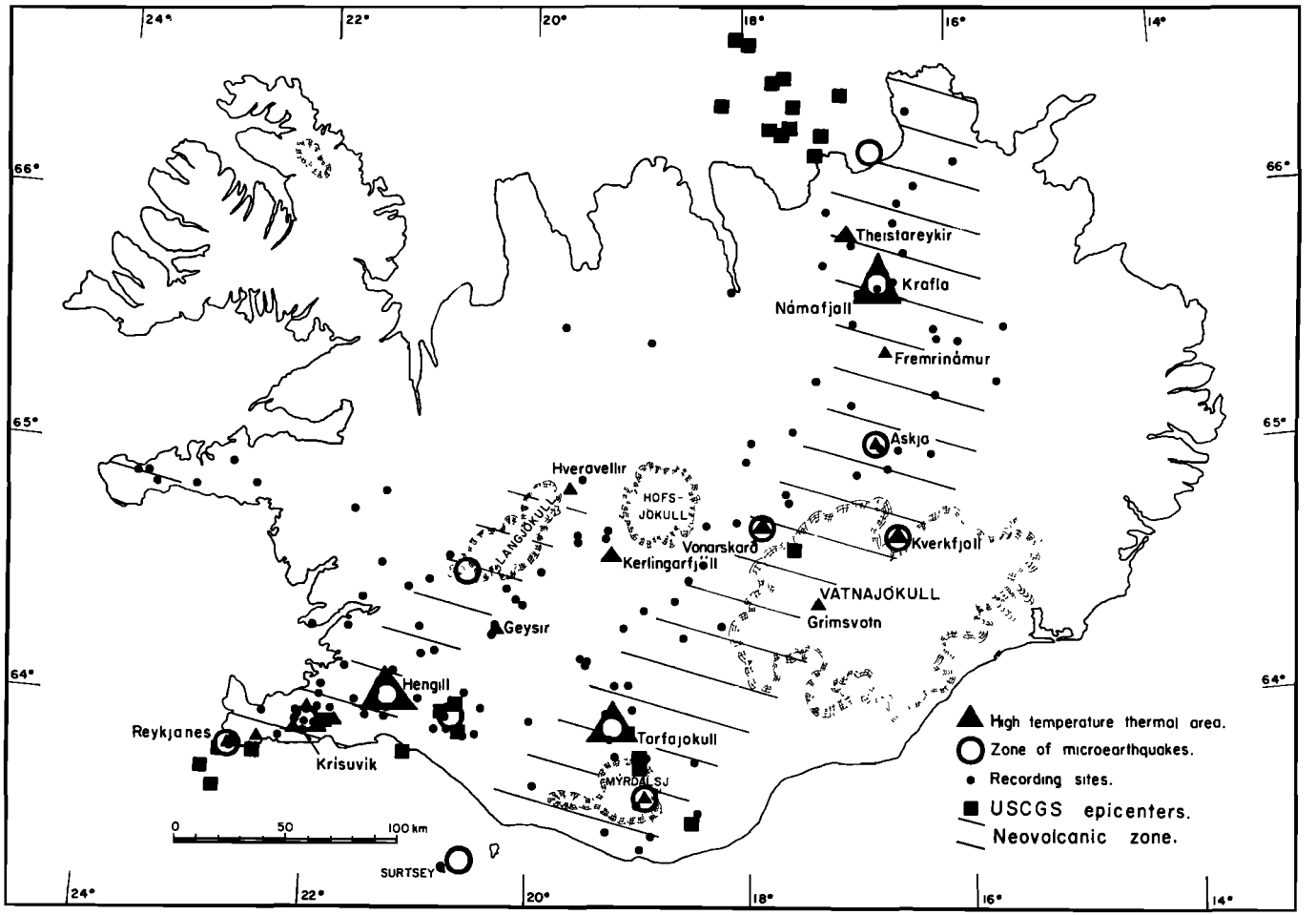


Fig. 1. Summary of microearthquake data and epicenters reported by the U. S. Coast and Geodetic Survey for 1967 through 1969. Jökulls are glaciers.

carthquake activity was observed in only a few relatively small regions. At most sites, no local events were recorded. Nine zones of activity can be located using the data collected in 1967 [*Ward et al.*, 1969]. The locations of six new zones that can be identified with the data for 1968 are summarized in Table 2. In this paper, two zones near Hveragerdi and one near Krísuvík located in 1967 [*Ward et al.*, 1969] are included as part of other zones nearby.

*Ward et al.* [1969] pointed out that the microearthquakes are spread over a much smaller area in Iceland than the larger earthquakes reported by many different sources. This results from the more accurate locations of the microearthquakes, but another factor may be a shift in the centers of activity with time.

It is somewhat surprising that the earthquakes occur in a few small zones generally less than 5 km in radius. In many studies, the microearthquakes are spread over a much larger area, often along faults [e.g., *Matumoto and Ward*, 1967; *Stauder and Ryall*, 1967; *Oliver et al.*, 1966; *Seeber et al.*, 1970]. This point will be discussed in the last section of this paper. The limited extent of the small zones is indicated by the small differences in $S$–$P$ times of events recorded at each recording site within or near a given zone of activity. Detailed locations of events in Hveragerdi and Krísuvík, discussed below, show that the active zones are indeed small, but these detailed studies do not rule out completely the possibility of minor microearthquake activity nearby.

*Temporal stability of the microearthquake activity.* Numbers of events per day are shown for data collected in 1967 in parentheses in Figure 3. The other numbers are for data from 1968. Only slight variations in activity were observed in most regions reoccupied after one year. *Ward et al.* [1969] observed that the

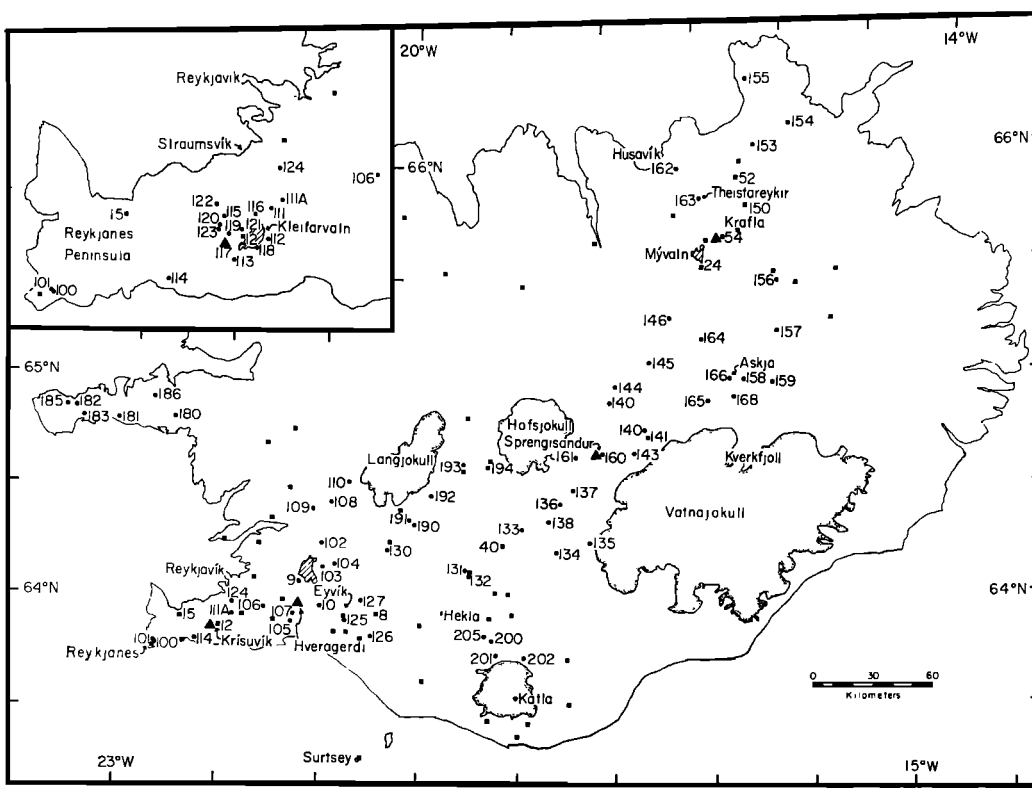


Fig. 2. Recording sites in Iceland. Numbers less than 99 denote sites occupied in 1967 and 1968. Numbers greater than 99 denote sites occupied in 1968. The dots without numbers next to them are sites occupied in 1967 only. Triangles are tripartite arrays. The insert shows more closely spaced sites on the Reykjanes Peninsula.

TABLE 1. Events Per Day Recorded at Each Site Occupied by Portable Seismometers*

| Sta. | Events/Day $S - P \leq 2.5$ sec | Events/Day $S - P > 2.5$ sec | Total Events Recorded | Hours with Noise 0.5 mm | Attenuation below Max. Gain | Date First Recorded |
|---|---|---|---|---|---|---|
| 8 | 0.6 (1.4) | 1.2 (1.4) | 7 | 41.2 | 24 | July 23 |
| 9 | 4.8 (0.7) | 0.8 (1.4) | 45 | 94.0 | 24, 30 | 7 |
| 10 | 0.8 (22.9) | 0.3 (0.6) | 16 | 88.6 | 24, 30 | 23 |
| 12 | 17.1 (13.6) | 0.8 (0) | 210 | 86.0 | 18, 24, 30 | 3 |
| 12 | 0.0 | 1.9 (8.0†) | 73 | 102.1 | 24, 30 | 15 |
| 15 | 0.0 (0.6) | 6.0 (0.0) | 8 | 32.0 | 30 | 3 |
| 15 | 0.0 | 5.3 | 3 | 13.0 | 30 | 17 |
| 24 | 0.0 (0.0) | 0.0 (0.0) | 0 | 48.4 | 0, 12 | Aug. 5 |
| 40 | 0.0 (0.0) | 1.9 (9.0†) | 3 | 36.9 | 24 | July 28 |
| 52 | 0.0 (0.0) | 0.0 (1.8) | 1 | 17.4 | 30 | Aug. 6 |
| 54 | 1.2 (191.0) | 0.0 (0.0) | 20 | 39.9 | 18 | 4 |
| 100 | 12.6 | 0.0 | 20 | 38.0 | 36 | July 3 |
| 101 | 18.6 | 0.0 | 19 | 24.5 | 36 | 5 |
| 102 | 0.0 | 1.0 | 7 | 99.4 | 18, 24, 30 | July 6 |
| 104 | 0.0 | 0.4 | 11 | 184.5 | 24, 30 | 7 |
| 105 | 3.2 | 0.0 | 3 | 15.0 | 30 | 7 |
| 106 | 0.7 | 1.8 | 15 | 67.0 | 24, 30 | 7 |
| 107 | 0.2 | 0.2 | 11 | 40.0 | 30 | 9 |
| 108 | 0.8 | 0.2 | 18 | 87.1 | 24, 30 | 11 |
| 109 | 0.0 | 1.3 | 7 | 18.0 | 18 | 11 |
| 110 | 6.9 | 0.0 | 101 | 69.8 | 24, 30 | 12 |
| 111 | 3.2 | 1.3 | 14 | 38.0 | 18, 24 | 15 |
| 111A | 5.9 | 0.3 | 43 | 85.1 | 12, 24, 30 | 17 |
| 112 | 11.6 | 2.2 | 145 | 99.3 | 18, 24, 30 | 15 |
| 113 | 2.8 | 0.0 | 3 | 25.0 | 30 | 16 |
| 114 | 6.1 | 0.5 | 24 | 43.7 | 30 | 17 |
| 115 | 2.8 | 0.0 | 7 | 34.3 | 24, 30, 36 | 19 |
| 116 | 4.0 | 8.5 | 48 | 42.5 | 24, 30 | 19 |
| 117 | 20.7 | 18.0 | 89 | 35.9 | 30 | July 20 |
| 118 | 13.1 | 23.4 | 90 | 32.9 | 24, 30 | 20 |
| 119 | 17.7 | 44.9 | 88 | 20.3 | 24 | 21 |
| 120 | 2.9 | 11.7 | 52 | 32.9 | 24, 30 | 21 |
| 121 | 12.1 | 0.0 | 13 | 11.9 | 30 | 22 |
| 122 | 1.9 | 0.0 | 2 | 12.8 | 30 | 22 |
| 123 | 1.9 | 0.0 | 3 | 12.6 | 30 | 22 |
| 124 | 0.0 | 0.0 | 0 | 7.5 | 24 | 22 |
| 125 | 1.4 | 1.8 | 18 | 67.2 | 18, 24, 30 | 23 |
| 126 | 1.0 | 1.5 | 6 | 49.2 | 12, 30 | 23 |
| 127 | 0.0 | 0.9 | 1 | 19.7 | 30 | 23 |
| 130 | 0.0 | 0.0 | 0 | 42.4 | 24, 30 | 25 |
| 131 | 0.0 | 0.0 | 2 | 21.9 | 18, 24 | 28 |
| 132 | 0.0 | 0.0 | 0 | 10.3 | 18 | 28 |
| 133 | 0.0 | 1.2 | 6 | 41.9 | 18, 24, 30 | 29 |
| 134 | 0.0 | 0.0 | 0 | 42.3 | 6, 18 | July 29 |
| 135 | 0.0 | 0.0 | 0 | 38.5 | 12 | 29 |
| 136 | 0.0 | 0.0 | 0 | 16.7 | 18 | 31 |
| 137 | 0.0 | 0.0 | 1 | 10.0 | 18 | 31 |
| 138 | 0.0 | 0.0 | 0 | 13.8 | 18 | 31 |
| 140 | 0.0 | 0.0 | 0 | 43.8 | 12, 18 | Aug. 1 |
| 141 | 0.0 | 0.0 | 2 | 28.4 | 18 | 1 |
| 142 | 0.0 | 0.0 | 2 | 29.5 | 18, 24 | 2 |
| 143 | 4.4 | 0.0 | 6 | 16.4 | 30 | 2 |
| 144 | 0.0 | 0.0 | 0 | 19.0 | 18 | 3 |
| 145 | 0.0 | 0.0 | 0 | 22.1 | 30 | 3 |
| 146 | 0.0 | 0.0 | 0 | 23.5 | 30 | 3 |
| 150 | 0.0 | 0.0 | 0 | 64.1 | 24 | 6 |
| 153 | 0.7 | 2.6 | 39 | 58.0 | 12, 18, 24 | 7 |

TABLE 1. (*continued*)

| Sta. | Events/Day $S - P \leq 2.5$ sec | Events/Day $S - P > 2.5$ sec | Total Events Recorded | Hours with Noise 0.5 mm | Attenuation below Max. Gain | Date First Recorded |
|---|---|---|---|---|---|---|
| 154 | 0.0 | 0.4 | 18 | 29.0 | 12, 24 | 7 |
| 155 | 0.0 | 2.5 | 39 | | 6 | 8 |
| 156 | 0.0 | 0.0 | 1 | 22.0 | 12 | Aug. 10 |
| 157 | 0.0 | 0.0 | 0 | 42.7 | 24 | 10 |
| 158 | 2.2 | 0.0 | 54 | 66.5 | 6 | 10 |
| 159 | 0.7 | 0.0 | 2 | 36.5 | 18, 24 | 12 |
| 160 | 0.0 | 1.3 | 2 | 17.8 | 18, 24 | July 29 |
| 161 | 0.0 | 0.0 | 5 | 73.3 | 6, 12 | 30 |
| 162 | 0.6 | 0.6 | 28 | 74.3 | 6, 12, 18 | Aug. 6 |
| 163 | 0.0 | 0.0 | 5 | 80.1 | 6, 12, 18 | 6 |
| 164 | 0.0 | 0.0 | 0 | 48.0 | 0 | 10 |
| 165 | 0.5 | 2.0 | 49 | 49.0 | 12, 18 | 10 |
| 165A | 0.0 | 0.0 | 3 | 20.2 | 18 | 14 |
| 166 | 1.7 | 0.0 | 5 | 14.0 | 12 | 14 |
| 168 | 0.0 | 0.0 | 1 | 17.4 | 6 | 14 |
| 180 | 0.0 | 0.0 | 0 | 64.9 | 18, 24 | 19 |
| 181 | 0.0 | 0.0 | 1 | 61.3 | 12, 18, 24 | 19 |
| 182 | 0.0 | 0.0 | 0 | 9.0 | 18 | Aug. 19 |
| 183 | 0.0 | 0.0 | 0 | 27.5 | 24 | 19 |
| 185 | 0.0 | 0.0 | 0 | 30.8 | 24 | 20 |
| 186 | 0.0 | 0.0 | 0 | 19.4 | 18 | 21 |
| 190 | 0.0 | 0.0 | 0 | 81.2 | 12, 18 | 23 |
| 191 | 0.0 | 0.0 | 0 | 45.5 | 24 | 23 |
| 192 | 0.0 | 0.0 | 7 | 32.0 | 6 | 23 |
| 193 | 0.6 | 0.0 | 2 | 39.0 | 6, 24 | 23 |
| 194 | 0.0 | 0.0 | 0 | 19.0 | 30 | 26 |
| 200 | 1.2 | 0.0 | 31 | 60.5 | 18 | 28 |
| 201 | 0.0 | 0.0 | 0 | 37.8 | 6, 12 | 28 |
| 202 | 0.0 | 0.0 | 0 | 15.0 | 12 | 29 |
| 205 | 0.0 | 0.0 | 0 | 16.9 | 18 | 30 |

* Number in parentheses are for data collected in 1967.
† Includes known aftershocks or swarms [*Ward et al.*, 1969].

number of events per day at the same site on different days or at different sites equidistant from the same earthquake hypocenters could vary by as much as a factor of 3. Most variations shown in Figure 3 are well within this limit. One exception is in southwestern Iceland, south of Eyvík, where substantially higher numbers were recorded in 1967. Observation in this region was begun, however, significantly to record aftershocks of a magnitude 5 earthquake on July 27, 1967. Thus, the high rate is probably atypical.

The most notable exception is at the volcano Krafla in northeastern Iceland, where 191 events per day were recorded in 1967 and only 1.2 events per day in 1968. It is possible that the events in 1967 were aftershocks of an event of magnitude 3 to 4 recorded at Akureyri and Reykjavík days before the microearthquake recordings were made. This event was thought to occur between Mývatn and Húsavík, but the location is in doubt; it could have occurred near Krafla. This explanation for the high microearthquake activity seems implausible, however, because significant aftershock activity in southern Iceland observed for earthquakes of this magnitude rarely lasts longer than 12 hours.

Another explanation of the high rate in 1967 is that this rate corresponded to a swarm of earthquakes perhaps related to volcanic or geothermal activity. There was extensive volcanic activity in this region in the 1760's [*Thórarinsson*, 1960]. A solfatara field exists near the epicenters of these events, and the events occur in a major geothermal area. No matter what the explanation, this decrease of

microearthquake activity in the Krafla region by a factor of more than 150 between 1967 and 1968 illustrates that such large variations can occur but from the rest of the data appear to be rare.

The daily fluctuations in the number of events can be observed with data from a tripartite array operated nearly continuously at Hveragerdi between July 12 and September 4, 1968. The frequency distribution of daily counts is plotted in Figure 4. Only events with trace amplitudes greater than 18 mm are included. This amplitude cutoff was chosen by noting that at 18 mm the relation between the logarithm of the amplitude and the logarithm of the number of events with amplitude greater than or equal to that amplitude became nonlinear. This implies that some events with amplitudes less than 18 mm were missed in the count. The mean daily count for the 50 days was 3.6 events/day.

Sixty per cent of the recorded daily counts were between 2.0 and 5.9 and 80% were between 1.0 and 6.9. For daily counts based on two days' recording, 65% were between 2.0 and 5.9 events per day and for three days 70% were within these limits.

A Poisson's distribution, which would apply if the earthquakes occurred randomly in time, is shown by the solid line in Figure 4. Although the curve appears to fit the data, a test for goodness of fit shows that the fit is only significant at about the 50% level. The non-Poissonian distribution might be explained by the tendency for most of the microearthquakes in a given day to occur within a few hours and by the fact that there was a gradual decrease in activity during the summer.

These considerations of the daily and yearly fluctuations in the level of microearthquake activity show that the numbers given in Table 1 and Figure 3 are generally representative of

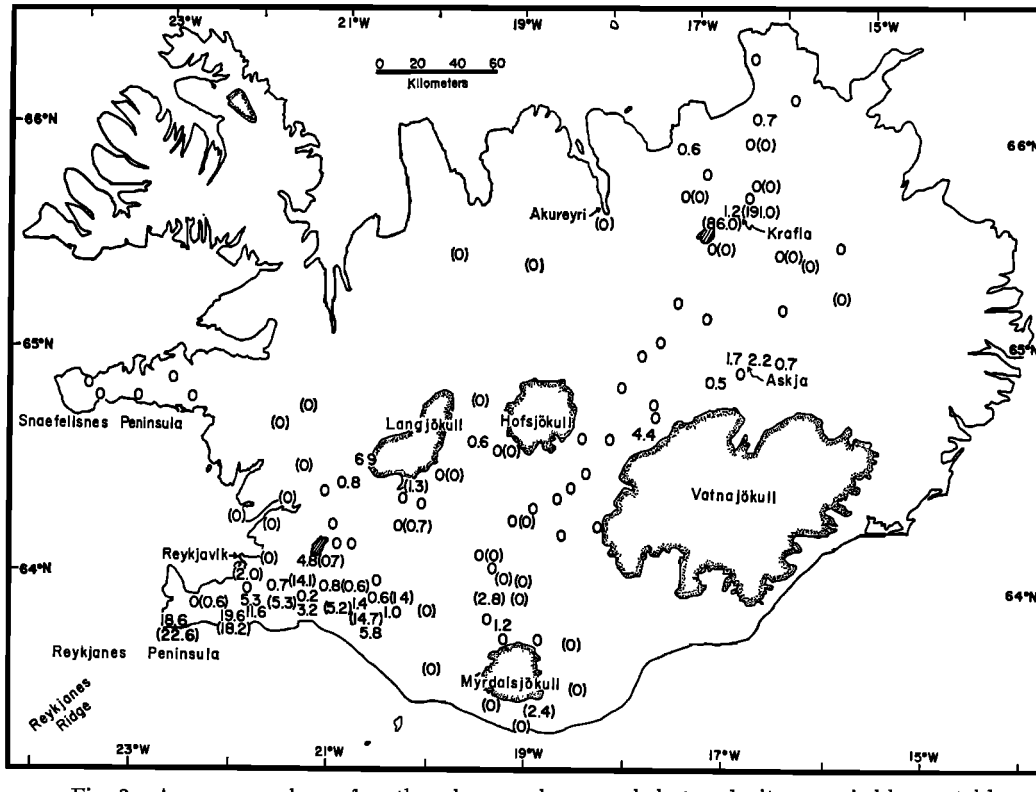


Fig. 3. Average numbers of earthquakes per day recorded at each site occupied by portable seismometers. Numbers in parentheses are data collected in 1967. The number is based on events with $S$–$P$ times $\leq 2.5$ sec and trace amplitudes $\geq 2$ mm at 30-db attenuation from maximum gain.

the activity as a function of time but that large variations can sometimes occur. It would be unreasonable, for example, to draw contours between the numbers in Figure 3 or to extrapolate them to find the long-term seismicity and expected occurrence of large earthquakes. If the numbers are based on two days of recording, there is about a 65% chance, according to the observations above, of that number being within ±45% of the daily mean for two months of recording. A survey of the type discussed in this paper does, however, give a general picture of the seismicity.

*Effect of attenuation on the number of microearthquakes observed.* The trace amplitudes and number of events recorded depend on the

TABLE 2. Location and Basis for Location of Six Zones of Microearthquakes

| Location of Zone | No. Events Recorded | Center of Zone | | Stations on Which Location Is Based | Quality of Location | Comments |
|---|---|---|---|---|---|---|
| | | Lat. N | Long. W | | | |
| NE of Surtsey | 63 | 63°36′ | 20°38′ | 8, 10, 125, 126, 127, Hveragerdi array | Located using stations >65 km away and at azimuths varying only by 20°. | 5–10 km NE of Surtsey, a volcanic island that first emerged above sea level in 1963 [*Thórarinsson*, 1967] and stopped erupting in June, 1967. *Norrman* [1969] reported many seamounts in this area. No microearthquake activity was observed in 1967, even though many sites were occupied along the coast nearby. |
| SW of Langjökull | 109 | 64°36′ | 20°38′ | 102, 108, 109, 110, Hveragerdi array | Stations only surround epicenters by 100°. Closest station 5 km away. | 3 events recorded in 1967 and located 11.5 km NW of station 46 [*Ward et al.*, 1969] may have been from this region. |
| E. edge of Askja | 21 | 65°1′ | 16°42′ | 158, 159, 165, 166, 168 | Well determined | Several fumaroles and solfatara fields occur here. *Tryggvason* [1970] observed tilting of the caldera floor. |
| Vonarskard | 4 | 64°43′ | 17°46′ | 143 | Poor location based only on $S - P$ time and the fact that no events were recorded at sites 141, 142, 162, and Sprengisandur array. | Earthquake ($M$ = 4.7) on November 8, 1968, located by USCGS at 64°36′ N and 17°18′ W. |
| Kverkfjöll | 43 | 64°42′ | 16°10′ | 158.165 | Location based on $S$–$P$ time and the fact that no events were recorded at site 164. | Numerous infrared anomalies in this region [*Friedman et al.*, 1969]. |
| Off coast N of Mývatn | 4 | 66°11′ | 16°48′ | 153, 154, 155, 162 | Well determined | Possibly aftershocks of event on July 30, 1968 ($M$ = 4.4), located by USCGS at 66°24′ N and 18°12′ W. |

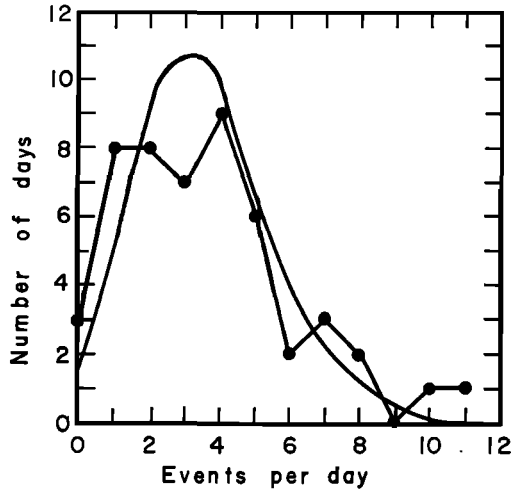


Fig. 4. The average number of earthquakes per day plotted against the number of days this average was observed at the Hveragerdi array. The curve is for a Poisson distribution with a mean of 3.6.

distance of the recorder from the hypocenters. To assess the effect of source distance, assume the earthquakes located near Krísuvík occurred in a small area and at an average depth of 3 km. Their locations will be discussed later, and it will be shown that this approximation is reasonable. The average numbers of events per day recorded at 13 sites is plotted in Figure 5 as a function of distance from the main cluster of earthquakes. The small dots in Figure 5 indicate the daily counts based on 8 to 25 hours of recording. The large dot is the average based on all events recorded during periods of low background noise divided by the total hours of low noise recording time. The amplitude and *S–P* time cutoffs are 2 mm and 2.5 sec, respectively.

Theoretically the amplitude might be expected to decrease with distance according to the formula [*Gutenberg*, 1959]

$$A = A_0 X^{-1} \exp(-\pi f X/QV) \qquad (1)$$

where $A_0$ is a constant, $X$ is the distance, $f$ is the predominant frequency, $V$ is the $P$-wave velocity, and $Q$ is a coefficient dependent on the anelastic properties of the rock. The $X^{-1}$ term represents geometrical spreading of body waves, and the exponential term is for anelastic attenuation. Other forms of attenuation equations have been suggested [e.g., *Asada*, 1957; *Romney*, 1959]. The differences in these equations are insignificant for the purposes of this study.

The number of events $[n(A)]$ with amplitudes between $A$ and $A + dA$ is given by the following equations [*Ishimoto and Iida*, 1939]:

$$n(A)\,dA = CA^{-m}\,dA \qquad (2)$$

where $C$ is a constant. The cumulative number of events ($N$) with amplitudes greater than some minimum amplitude ($A_{min}$) observed at a station from a point source can be derived by integrating equation 2 with respect to the amplitude and substituting equation 1 for amplitude:

$$N = (C/bA_{min}^{b})[X^{-b} \exp(-bkX)] \qquad (3)$$

where $k = \pi f/QV$ and $b = m - 1$. For these data and other data in Iceland [*Ward et al.*, 1969], $b \approx 0.8$. The line in Figure 5 depicts $N$ where $f = 25$ cps, $b = 0.8$, $Q = 150$, $V = 2.8$

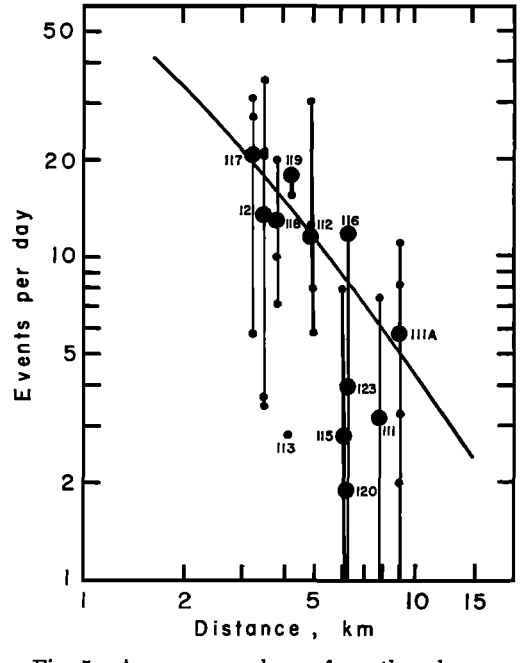


Fig. 5. Average number of earthquakes per day versus the distance of the station from the main source of earthquakes at Krísuvík. Vertical lines show the variation in daily counts. The large dots are the over-all averages for each station. The curve is the predicted decrease in number taking geometrical spreading and anelastic attenuation into account.

$+ 0.11X$, and $C/bA_{min}^{b} = 8.0$. The fit to the data is as good as can be expected. If $Q$ equals 50, the curve nearly passes through points 117 and 115. Thus, $Q$ must be low, or the attenuation must be high, if the four data points from stations 111, 115, 120, and 123 are to lie along the same curve as the data from stations closer to the source. If these four stations are omitted, a $Q$ of up to 500 will fit the data reasonably well.

The low daily counts at these four stations might be explained by the radiation pattern. This is not so, however, if all the microearthquakes are assumed to have the same focal mechanism as the major earthquake of December 5, 1968, located about 15 km east of this area [*Ward*, 1970]. The observed first motions generally support this assumption about the focal mechanism. Stations 121, 12, 112, and 118 are closest to the $P$-nodal planes, but these stations do not have lower daily counts than other stations at the same distance. Other effects such as local geologic structure, differences of geophone foundations, etc., could influence the daily counts. The ray paths from the source to stations 115, 120, and 123 travel across a lava-filled graben to the northwest of the major source of activity. The attenuating effect of such a graben in Iceland was pointed out by *Ward et al.* [1969]. The daily count of events recorded is thus a function of source distance and local geologic structure, as well as seismic activity.

*Relative activity of the 13 microearthquake zones.* The number of events that would be recorded if the instruments were within a certain distance from a particular source can be predicted by applying equation 3. If the earthquakes are assumed to occur in a very small volume and if, for example, the daily counts are to be normalized to the value that would be observed if all stations were 3 km from the source, then from equation 3 the number of events ($No$) at this distance is

$$No = NX^{b}3^{-b} \exp [kb(X - 3)] \quad (4)$$

The normalized numbers using the data from the station closest to a particular zone are given in Table 3. Numbers in parentheses are less reliable because the daily counts are small and the distances involved are large. Clearly the area northeast of Surtsey had very high activity, even if the normalization procedure is incorrect by a factor of 5. This activity is apparently greater than that observed near Krafla in 1967.

The normalization factor at 30 km distance is 40. Thus, for one event to be recorded at this distance in two days, the microearthquake zone must have a normalized activity, as described above, of about 20 events per day. Seven of the 13 zones located in this study have

TABLE 3. Normalization of the Daily Count of Earthquakes for an $S$–$P$ Time of 0.5 Seconds*

| Earthquake Zone | Instrument Site | Daily Count | Average $S - P$ Time | Normalization Factor | Normalized Daily Count | Quality of Observation |
|---|---|---|---|---|---|---|
| Reykjanes | 101 | 18.6 | 0.8 | 2.6 | 48 | Good |
| Krísuvík | 12 | 22.9 | 0.8 | 2.6 | 60 | Good |
| Hengill-Hveragerdi | 9 | 4.8 | 1.7 | 7.6 | 36 | Good |
| Langjökull | 110 | 6.9 | 0.7 | 2.2 | 15 | Fair |
| SE of Hengill | 125 | 1.4 | 0.6 | 1.1 | 2 | Good |
| Surtsey | 126 | 1.5 | 8.5 | (172) | (258) | Fair |
| Katla | 4† | 2.4 | 2.0 | 12.6 | 30 | Poor |
| N of Mýrdalsjökull | 200 | 1.2 | 0.7 | 2.2 | 3 | Fair |
| Vonarskard | 143 | 4.4 | 0.4 | 0.8 | 4 | Poor |
| Askja | 158 | 2.2 | 1.0 | 3.8 | 8 | Good |
| Kverkfjöll | 165 | 0.9 | 4.0 | (45) | (40) | Poor |
| In the ocean N of Mývatn | 153 | 1.5 | 2.0 | 12.5 | 19 | Fair |
| Krafla | 54 | 1.2 | 0.4 | 1.0 | 1 | Good |

* Numbers in parentheses are less reliable because the daily counts are small and the distances are large.

† 1967.

normalized counts of less than 20 events per day. Although the recording sites were spread throughout most of Iceland, large parts of eastern and northwestern Iceland are more than 30 km from any recording site. This distance limit is minimized in many cases, since at most sites several recorded events were smaller in size than those considered in the daily count. The amplitude limit for the daily count was chosen as the lowest amplitude that could be observed at all sites. Furthermore, when an event was located during the field work, instruments were moved close to the epicenter if possible. Nevertheless, it must be concluded that activity outside the neovolcanic zone and outside the Snaefellsnes Peninsula could have been missed. In addition, activity similar to that observed in 7 of the 13 zones could have been missed in parts of the neovolcanic zone. These considerations demonstrate clearly the necessity of operating portable seismometers at many different sites for studies of the type discussed in this paper.

*Significance of the locations of microearthquake zones.* Nine of the thirteen zones of microearthquake activity occur in regions of major geothermal activity. Two of the remaining zones occur in regions of historic submarine volcanism where geothermal activity may exist. One zone is near Surtsey, a volcanic island off the coast of south-central Iceland that erupted from 1963 to 1967 [*Thórarinsson,* 1967]. Numerous seamounts have been observed in the region near this volcano [*Norrman,* 1969], suggesting other sites of submarine volcanism. Historic volcanism has also been reported near the microearthquake zone in the ocean north of Mývatn in northeastern Iceland [*Beninghausen,* 1964; *Thórarinsson,* 1967]. The microearthquake zone southeast of Hveragerdi coincides with the epicenters of three magnitude 4 to 5 earthquakes. Thus the microearthquakes might be considered as foreshocks and aftershocks. The fourth microearthquake zone not associated with known geothermal activity occurred on the southwestern edge of Langjökull near an acidic intrusion.

One of the most significant observations of this study is that the majority of the observed microearthquakes occurred in major geothermal areas. Major geothermal areas [*Bödvarsson,* 1961] are characterized at the surface by numerous fumeroles, large regions of hot ground, and a high degree of thermal alteration. Heat output in each area ranges from 5 to 750 $\times$ $10^6$ cal/sec, and the subsurface temperatures are from 200° to 290°C. Several properties of the major geothermal areas in Iceland are summarized in Table 4, together with the microearthquake data. Some data in this table were taken from *Bödvarsson* [1961], *Arnórsson* [1969], *Arnórsson et al.* [1969], and Saemundsson (personal communication, 1970).

Nine of the seventeen major geothermal areas in Iceland had significant microearthquake activity when studied in 1967 and 1968. Instruments were not placed close enough to four of the other eight areas to sample sufficiently the microearthquake activity. As is shown in Table 4, three areas, Geysir, Hveravellir, and Kerlingarfjöll, have no observed microearthquake activity and, unlike the other areas, do not appear to be related to fissure systems. Furthermore, all three areas have thermal waters with fluorine concentrations in excess of 1.5 ppm. High fluorine concentration is characteristic of alkaline waters flowing from regions with acidic volcanics [*Arnórsson,* 1969]. This relationship is complicated somewhat because the total amount of fluorine is influenced by the solubility of fluorspar and is therefore in inverse proportion to the amount of calcium in the water. In any case, the geothermal areas that have no observed microearthquake activity might be considered to be dominated structurally by acidic intrusions, whereas those areas with microearthquake activity are structurally related to fissure systems trending parallel to the strike of the neovolcanic zone. The one exception to this generalization is Theistareykir (in northeastern Iceland), which has no observed microearthquake activity but does seem related to fissures.

One method of identifying emission of heat at the surface is with infrared surveys. *Friedman et al.* [1969] used an airborne line-scanning system to measure infrared radiation emitted from several regions in Iceland that were known to have some thermal activity. At Krísuvík, high infrared emission was found in the southern part of Kleifarvatn and to the southwest in the area just north of Krísuvík. High emission was also observed near Reykjanes, Kverkfjöll, Askja, and Krafla. The only

TABLE 4. Major Geothermal Areas in Iceland Listed by Location from Southwest to Northeast*

| Area | Approx. Area, km² | Approx. Natural Heat Output, × 10⁶ cal/sec | Elevation, meters | Dominating Structural Features | | | | Acid Rocks at Surface | Approx. Fluorine Content of Water, ppm | Normalized No./Day | Quality of Observation | Distance, nearest km |
|---|---|---|---|---|---|---|---|---|---|---|---|---|
| | | | | Fissures | Calderas | Shield Volcanoes | Explosion Craters | | | | | |
| 1. Reykjanes | 2 | 5–25 | 20 | × | | | | None | 0.2–0.3 | 48 | Good | 1 |
| 2. Svartsengi | 1 | 5–25 | 30 | × | | | | None | ? | ? | Poor | 8 |
| 3. Krísuvík | 50 | 25–125 | 160 | × | | | × | None | 0.3–0.4 | 60 | Good | 1 |
| 4. Brennisteinsfjöll | 1 | 5–25 | 600 | × | | | | None | ? | ? | Poor | 7 |
| 5. Hengill-Hveragerdi | 90 | 25–125 | 30–400 | × | | | × | Some | 0.2–2.6 | 36 | Good | 1 |
| 6. Geysir | 1 | 5–25 | 120 | | | | | Some | 9.5–12 | 0 | Good | 1 |
| 7. Hveravellir | 1 | 5–25 | 600 | | | × | | Some | 2–4 | 0 | Good | 1 |
| 8. Kerlingarfjöll | 10 | 25–125 | 950 | | | | | Major | 1.5? | 0 | Fair | 4 |
| 9. Katla | ? | ? | 1100 | ? | ? | | | Some | ? | (30) | Poor | 18 |
| 10. Torfajökull | 150 | 125–750 | 600–1000 | × | ? | | × | Major | ? | 3 | Fair | 7 |
| 11. Vonkarskard | 10 | 5–25 | 1000 | ? | | | | Some | 0.3–27 | 4? | Poor | 9 |
| 12. Grímsvötn | 20? | 125–750? | 1340 | ? | × | | | ? | ? | ? | Poor | 45 |
| 13. Kverkfjöll | 5 | 5–25 | 1700 | × | | | | ? | ? | 40 | Good | 30 |
| 14. Askja | 5? | 5–25 | 1050 | × | × | | × | Some | ? | 8 | Good | 3 |
| 15. Fremrinámur | 2 | 5–25 | 800 | × | | × | | Some | ? | ? | Poor | 24 |
| 16. Námafjall-Krafla | 60 | 25–125 | 350–560 | × | | × | × | Some | 0.5–1.5 | 1(191) | Good | 1 |
| 17. Theistareykir | 20 | 25–125 | 340 | × | | × | | Some | ? | 0 | Fair | 1 |

* Locations are shown in Figure 1. Earthquake data in parantheses were collected in 1967; other data were collected in 1968.

areas surveyed by Friedman et al. but found in this study to have low microearthquake activity were Hekla, in south-central Iceland, and the Theistareykir geothermal area, north of Mývatn. Hekla is a volcano that erupted in 1947 [*Thórarinsson*, 1967] and in 1970. Infrared anomalies were found on Surtsey, a volcano that erupted in 1967, and earthquakes were located to the northeast. The poor accuracy of the epicentral locations, however, and the difference in times of the two different types of surveys do not permit detailed correlation.

*Transform faults in Iceland.* The zones of microearthquake activity in Iceland all occur within the zone of active rifting and volcanism. Furthermore, six of the zones lie along an east-west trend in southern Iceland. *Ward et al.* [1969] discuss the possibility of a transform fault along this trend near 64°N. *Ward* [1971*a*] summarizes the distribution of microearthquakes presented here, together with the historic seismicity, focal mechanisms, and the geology of Iceland to show that the fracture zone probably strikes west-northwest and may be 80 km wide.

## PRECISE LOCATIONS OF SOME MICROEARTHQUAKES IN ICELAND

In addition to the general survey of microearthquakes in Iceland, two tripartite arrays were used in 1968 to locate some microearthquakes with precisions of ±0.6 to 1.0 km in depth and distance. It was shown above that most major geothermal areas in Iceland had high microearthquake activity. The detailed locations discussed below of events in the geothermal areas near Krísuvík and Hengill-Hveragerdi in southwestern Iceland show a close spatial correlation between the epicenters of microearthquakes and geothermal activity observed at the surface. Most of the well-located microearthquakes occurred at 2 to 6 km depth in the uppermost part of layer 3, a crustal layer with $P$-wave velocity of about 6.5 km/sec. Some less well located events were as deep as 13 km. In this section, the instrumentation and hypocentral accuracy are briefly described. The earthquake locations are presented and are related briefly to local structural lineaments, geothermal features, and crustal layer 3. The reasons for these relationships are discussed in a later section.

*Instrumentation.* The location, dimensions, and duration of recording for each array are summarized in Table 5. The Hveragerdi array consisted of three Geospace (HS-10) 2-cps vertical geophones, three Electro-Tech (SPA-1) amplifiers, and a Geotech (Model 17373) tape recorder operating at 15/160 ips. The array operated at Krísuvík, Sprengisandur, or Krafla consisted of three Dayton 4.5-cps vertical geophones, three Electro-Tech amplifiers, and a Precision Instrument (Model 5104) tape recorder operating at 3/8 ips. Sprengnether (TS-100) chronometers were used. Absolute timing accuracy was not required for locations at each array. Local earthquakes were recorded at all

TABLE 5. Location, Surveyed Size, and Dates of Operation of the Tripartite Arrays*

| Station | Lat. N | Long. W | Length, km | | Elevation, km | | Angle | Angle North to Line | Dates in |
|---|---|---|---|---|---|---|---|---|---|
| | | | *A-B* | *A-C* | *A-B* | *A-C* | *BAC* | *A-B* | Operation |
| Hveragerdi | 64.04° | 21.21° | 0.9332 | 1.1126 | −0.022 | −0.109 | 101.87° | 213.0° | July 12 to Sept. 4, Sept. 11 to Oct. 5 |
| Krísuvík | 63.91° | 22.01° | 1.1772 | 1.4409 | −0.075 | −0.006 | 71.34° | 221.7° | July 13 to July 23,† Aug. 19 to Sept. 3† |
| Krafla | 65.68° | 16.81° | 1.2331 | 1.4277 | −0.070 | −0.054 | 72.49° | 320.9° | Aug. 5 to Aug. 16 |
| Sprengi-sandur | 64.75° | 18.09° | | | | | | | July 30 to Aug. 4 |

* The geophones are defined as $A$, $B$, and $C$ in a clockwise sense (P. L. Ward, unpublished data, 1971).
† Recording was discontinuous because of instrument problems.

sites except Sprengisandur, which will not be discussed further.

*Hypocenter accuracy.* The techniques and precision involved in using tripartite arrays to locate local earthquakes are discussed in detail by *Ward* [1971*b*]. In that paper it is shown that possible errors resulting from uncertainties in reading arrival times can be excessive at certain distances and azimuths because of array geometry. Thus, it is important to calculate the possible errors in the locations of different events. If proper care is taken when setting up an array and analyzing the data, the precisions in reading the relative times of the first arrivals of the *P* waves and *S* waves are the most significant errors in determining the precisions of the calculated hypocenters. In this work, *P*-wave arrivals could be read to within ±0.2 mm on the strip-chart records using a table-top digitizer. This distance corresponds to ±0.006 sec for the Hveragerdi array and ±0.003 sec for the other arrays. The first arrivals of the *S*-wave are often difficult to distinguish. In this work, errors in reading the *S*-wave arrival time vary from ±0.01 to ±0.1 sec.

Throughout the recording period at Hveragerdi, large explosions were detonated for harbor construction at Straumsvik, 38.6 km west of the array. Of the 114 well-recorded explosions, 83% of the calculated azimuths and 81% of the apparent velocities were within their error limits, equal to 313.5 and 11.6 km/sec, respectively. If the error in reading the *P*-wave arrival was ±0.008 sec at Hveragerdi, instead of ±0.006 sec as assumed, all events would be within the maximum error limits. This discrepancy can be explained by slight changes (±0.05 mm) in the alignment of each trace across the strip chart records (P. L. Ward, unpublished data, Figure 14, 1971) that were produced over several weeks as the tapes were played back. The galvanometers in the Siemans Oscillomink recorder, used in this study, must be carefully adjusted so that the traces line up across the chart. The important point is that the calculated precisions given in this paper should be considered as the 80% confidence limits.

Crustal structures within linear velocity gradients for each array are shown in Table 6. These structures were calculated starting with crustal models consisting of layers of constant velocity and travel time data provided by *Pálmason* [1963, 1967*b*, 1970] (personal communication, 1969). Velocity gradients were introduced and the layering was modified until the calculated travel times fit the observed travel-time data. Reversed travel-time profiles were not available in the regions near the arrays. Pálmason (personal communication, 1969) suggested, however, that the layers may dip a few degrees in the profiles studied. A number of explosions were detonated near the arrays to examine the accuracy of the calculated locations (Table 7). The crustal structures were finally modified to make the observed and calculated apparent velocities agree for those explosions with equal observed and calculated azimuths. The structures given in Table 6 are not the only ones that fit the data. The structure for Krísuvík is the best determined. *S*-wave velocities were calculated from the *P*-wave velocities assuming a Poisson's ratio of 0.28 [*Pálmason*, 1963].

TABLE 6. Crustal Structures

| Station | *P* Vel. at Top of Layer, km/sec | Thickness, km | Gradient, km/sec/km |
|---|---|---|---|
| Krísuvík | 2.2 | 0.1 | 8.0 |
| | 3.0 | 0.5 | 1.2 |
| | 3.6 | 2.2 | 1.18 |
| | 6.2 | 3.5 | 0.28 |
| Hveragerdi | 2.75 | 1.1 | 1.47 |
| | 4.37 | 1.0 | 1.02 |
| | 5.4 | 2.0 | 0.50 |
| | 6.4 | 6.0 | 0.12 |
| Krafla | 2.2 | 0.3 | 3.00 |
| | 3.1 | 1.5 | 1.33 |
| | 5.1 | 2.0 | 0.34 |
| | 5.8 | 2.0 | 0.34 |

*Effect of dipping crustal layers on hypocenter locations determined from data from a tripartite array.* The calculated azimuths and apparent velocities for explosions more than 18 km from the Hveragerdi array vary as much as 38° and a factor of 1.6, respectively, from those predicted for the known locations (Table 7). The calculated locations of a number of earthquakes recorded from the microearthquake zones discussed above also showed this discrepancy. These data are summarized in Table 8. These large errors, as is shown below, can

TABLE 7. Calculated and Actual Locations of Explosions Used to Calibrate the Tripartite Arrays

| Array | True Azimuth | Calc. Azimuth* | Theoret. Appar. Vel., km/sec | Calc. Appar. Vel., km/sec | True Distance, km | Calc. Distance, km | Calc. Depth, km |
|---|---|---|---|---|---|---|---|
| Krafla | 16° | 30.1° (±1.2) | 4.37 | 4.36 (±0.07) | 4.7 | 5.1 (4.7–5.2) | 0.0 (0.2–0.0) |
| Krísuvík | 9° | 353.3° (±1.9) | 6.31 | 7.19 (±0.23) | 15.5 | 17.3 (17.2–17.7) | 6.2 (7.8–4.1) |
| Krísuvík | 63° | 64.9 (±0.9) | 5.06 | 5.19 (±0.14) | 7.0 | 7.0 (6.6–7.2) | 0.4 (0.5–0.0) |
| Krísuvík | 164° | 162.3° (±1.2) | 3.46 | 3.49 (±0.04) | 3.1 | 3.1 (2.9–3.1) | 0.1 (0.2–0.0) |
| Krísuvík | 329° | 328.8° (±0.9) | 3.09 | 3.07 (±0.04) | 1.6 | 1.5 (0.5–1.7) | 0.0 (0.2–0.0) |
| Hveragerdi | 10° | 15.8° (±5.5)[a] | 6.6 | 5.68 (±0.55) | 26.0 | 23.7 (6.9–25.6) | 1.1 (5.8–0.0) |
| Hveragerdi | 78° | 68.8° (±2.2)[b] | 6.4 | 4.46 (±0.43) | 18.1 | 5.3 (3.2–6.8) | 0.0 (2.0–0.0) |
| Hveragerdi | 140° | 140.5° (±2.9) | 3.19 | 3.13 (±0.11) | 2.2 | 2.1 (1.2–2.1) | 0.0 (0.1–0.0) |
| Hveragerdi | 275° | 313.5° (±13.0)[c] | 7.2 | 11.62 (±1.5) | 38.5 | 32.8 (27.2–36.2) | 39.4 (44.3–0.1) |
| Hveragerdi | 349° | 351.0° (±7.0) | 5.48 | 5.66 (±0.29) | 10.3 | 12.3 (7.3–14.7) | 0.0 (2.0–0.0) |

* Calculated azimuth assuming station correlations given in text:

*a*. 4.3° (±8.4) *b*. 80.4 (±2.2) *c*. 280 0° (±5.9)

nearly all be explained, for example, by one layer at a depth of about 2 km in the crust dipping 2° to 5° in the region under the array. These data are of great importance to persons interested in detailed locations of local earthquakes, because they emphasize the need for using explosions or earthquakes located by a more accurate method to calibrate hypocentral locations determined with data from a tripartite array [*Ward*, 1971*b*].

If the crust is divided into laterally homogeneous layers of velocity, the azimuth from a tripartite array can be calculated independent of the velocity or velocity gradient in each layer. The calculation of expected apparent velocity for an explosion of known location, however, depends greatly on the assumed crustal structure. In many cases, the assumed structure can be modified to fit the observed apparent velocity data. For the data given in Tables 7 and 8, however, the apparent velocities are higher than predicted by the crustal model to the west of the array and lower than predicted to the east. Therefore, simply modifying the velocities and velocity gradients in the assumed crustal structure will not explain the differences between observed and predicted apparent velocities.

Perhaps the simplest explanation of these discrepancies is that lateral inhomogeneities in the crust under the array cause the first arrivals at one or two seismometers of the array to be delayed relative to the arrivals at the other one or two seismometers. In this case, station corrections should be added to the arrival times at each station to correct for such inhomogeneities. At Hveragerdi, however, explosions within 10.3 km were located accurately without assuming station corrections. Any station corrections that improve the accuracy of the more distant explosions reduce the accuracy of the local events. This fact suggests that any major lateral inhomogeneities near the array must occur at depths greater than 2 km, the depth to which rays in the assumed crustal structure (Table 6) travel between the array and a surface focus event about 10 km away. If only the data in Tables 7 and 8 for events more than 18 km from Hveragerdi are used to calculate station corrections by the least squares method outlined by *Ward* [1971*b*], then 0.056 sec should be subtracted from the arrival times at the

southernmost station of the array (station *B*, Table 5) and 0.019 sec should be subtracted from the arrivals at the westernmost station (station *C*). These time differences could be explained, for example, by an interface sloping about 2° to 5° to the southwest between two layers with a velocity contrast of 1 km/sec. A lower velocity contrast would give a higher dip. The strike of this interface would be northwest. Applying these station corrections makes most calculated azimuths agree, within their precision, with the known azimuths (Table 7) for explosions or interpreted azimuths (Table 8) for earthquakes.

The differences between observed and expected apparent velocities can also be explained by this simple model. If the interface between two layers is dipping away from the array, the apparent velocity will be higher than that for the horizontally layered case. If a layer is dipping toward the station, the apparent velocity will be lower. The apparent velocities in Tables 7 and 8 imply a dip to the southwest. This dip agrees with the dip deduced from the azimuthal data. The refraction data of *Pálmason* [1970] show a dip in the upper boundary of layer 3 in this region of about 2° or 3° to the southwest.

The effect of a dipping layer cannot be accurately taken into account by simply adding constant station corrections [*Niazi*, 1966]. A ray approaching the interface is refracted in three dimensions rather than in a two-dimensional plane between source and receiver, as is assumed in this work. The actual station corrections caused by a dipping layer would be a sinusoidal function of azimuth and would decrease with distance. The important point here is that a simple approximation explains nearly all the data. Any number of complications could be added to the model to make all the data fit. The rays, for example, may be reflected or refracted laterally at many points along their path.

Thus, very small inhomogeneities in the crustal structure can cause large errors in locations of earthquakes outside a tripartite array. For this reason, explosions or independently located earthquakes must be used to calculate the accuracy of array locations. The hypocentral locations given below are close to the respective arrays, and explosions near the arrays show that

TABLE 8. Calculated and Assumed Locations of Earthquakes Based on Hveragerdi Tripartite Array

| No. of Events | Azimuth | Assumed Azimuth | Calc. Azimuth* | Distance, km | Assumed Distance, km | Appar. Vel. km/sec | Theoret. Appar. Vel. km/sec | Area | Source of Assumed Location |
|---|---|---|---|---|---|---|---|---|---|
| 2 | 35–45° | 19° | 40–50° | 64–68 | 68 | 4.5–4.8 | 7.4–7.7 | West Geitlandsjökull | Stations 108, 110, 104 |
| 54 | 120–138° | 148–156° | 148–160° | 74–82 | 80 | 5.3–5.8 | 7.4–7.7 | 5–10 km NE of Surtsey | Stations 8, 10, 125, 126, 127 |
| 56 | 225–265° | | | 107–117 | | 14–20 | | Reykjanes Ridge | Krísuvík array |
| 22 | 262–320° | 252° | 255–262° | 40–44 | 41 | 10–12 | 7.2–7.3 | Kleifarvatn | Krísuvík array |
| 6 | 328–338° | 285–295° | 294–304° | 34–38 | 34–38 | 8.0–8.5 | 6.9–7.2 | Reykjavík | Krísuvík array, S–*P* |

* Assuming station corrections given in text.

the accuracy of these locations is nearly the same as the precision.

*Locations of microearthquakes near Hveragerdi.* Figure 6 shows epicenters of 315 local earthquakes recorded clearly at the Hveragerdi array in southwestern Iceland. Numbers denote depth to the nearest kilometer. This array was set up at the southern end of a large geothermal area. The easternmost seismometer was about 150 meters east of a large geothermal well that, as is discussed later, was opened and closed regularly during the summer to see if any change in the occurrence of microearthquakes could be noted. The precision of the earthquake locations in Figure 6 varies because of the geometry of the array. Figures 7, 8, 9, and 10 show the possible error in azimuth, apparent velocity, distance, and depth calculated by assuming errors in reading the $P$-wave arrivals and $S$–$P$ times of $\pm 0.005$ sec and $\pm 0.05$ sec, respectively, and plotted on a map similar to that in Figure 6. The errors are for earthquakes at a depth of 3 km. Distances from the array are measured from station $A$ (P. L. Ward, unpublished data, 1971), which in this case is arbitrarily defined as the easternmost

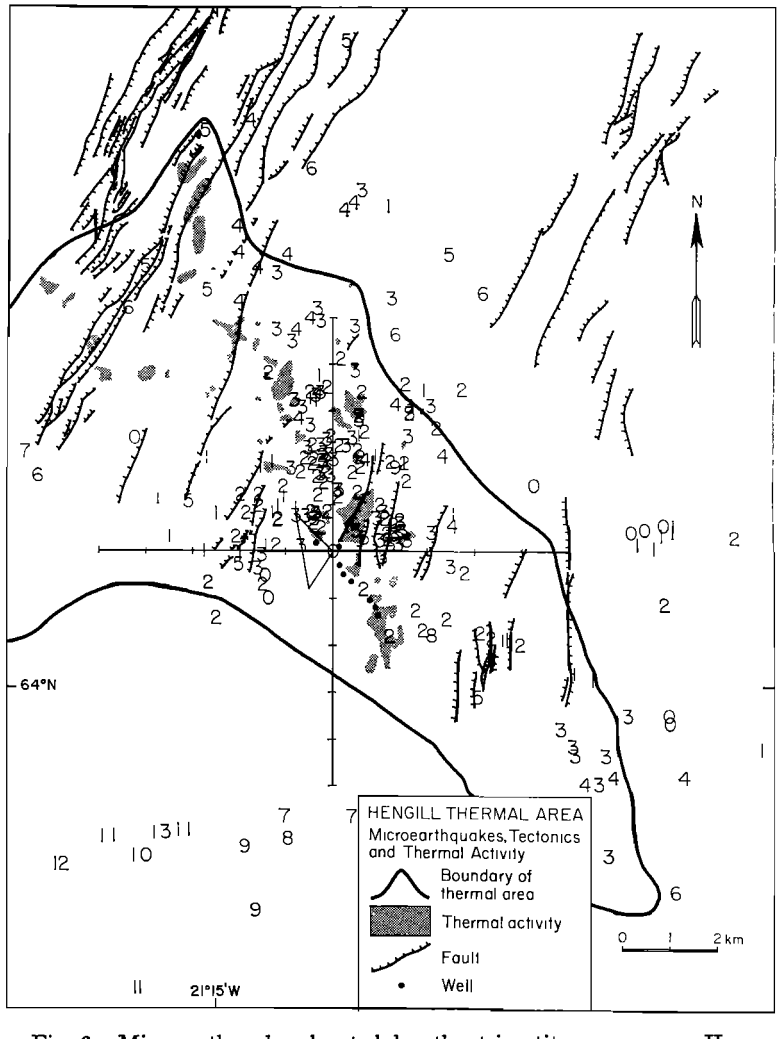


Fig. 6. Microearthquakes located by the tripartite array near Hveragerdi. Numbers denote depths to the nearest kilometer. The triangle is the array.

geophone. The errors are symmetrical about this point. The errors in azimuth and apparent velocity would decrease for shallower events at the same distance and would increase for deeper events. The errors in distance and depth would generally increase for shallower events and decrease for deeper events, although the relationship is more complex. Similar error maps for an equilateral array (P. L. Ward, unpublished data, 1971) show errors that are much more constant as a function of azimuth than those in Figures 7 to 10. Careful comparison of the error maps with the distribution of hypocenters plotted in Figure 6 shows that, when the possible errors are considered, many groups of hypocenters that appear scattered could have occurred at one point or along narrow linear trends. For example, seven of the ten events at depths of 3 and 4 km just 6 to 8 km southeast of the array could have occurred along one line.

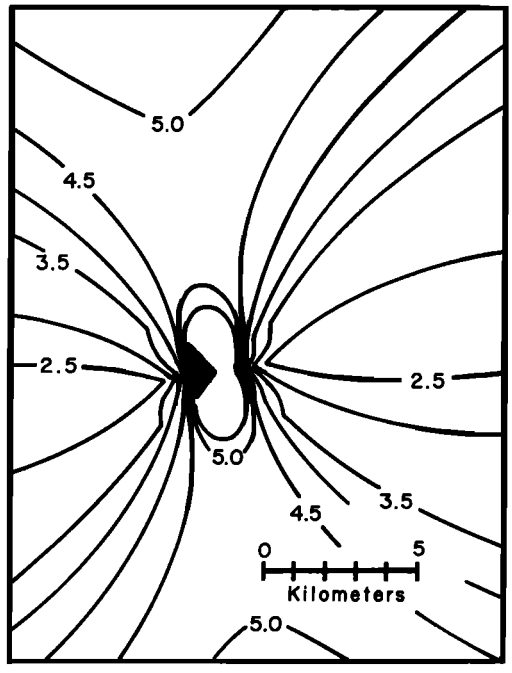


Fig. 7. Error in calculated azimuth from the Hveragerdi array plotted on the map shown in Figure 6. The numbers are the ± limits of the error in degrees and are calculated assuming an error in reading the $P$ arrivals of ±0.005 sec and an error in reading the $S$–$P$ arrivals at ±0.05 sec. All earthquakes are assumed to occur at 3 km depth. The triangle is the array.

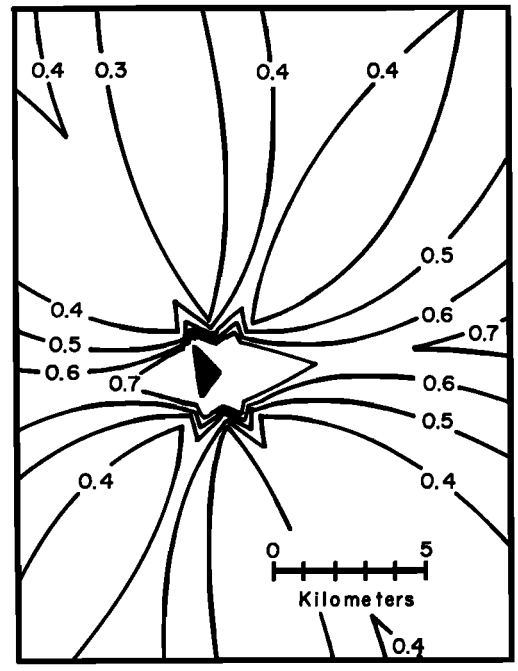


Fig. 8. Error in calculated apparent velocity plotted on the map shown in Figure 6. The numbers are the ± limits of the error in kilometers per second and are calculated assuming an error in reading the $P$ arrivals of ±0.005 sec and an error in reading the $S$–$P$ arrivals of ±0.05 sec. All earthquakes are assumed to occur at 3 km depth. The triangle is the array.

The five events 10 to 12 km deep southwest of the array could have occurred at one point. The apparent scatter of events beyond 2 km to the north of the array could be attributed to the possible errors in location, particularly to errors in azimuth.

The microearthquakes are primarily confined to the geothermal area defined by the occurrence of thermally altered rocks at the surface. The highest earthquake activity is near but not directly under the regions of thermal springs, fumaroles, etc. The fissures, grabens, and linear volcanic vents generally trend N30°E through the area. Some small groups of microearthquakes appear to have nearly the same trend, but this pattern is not very convincing. The more prominent S65°E trend just southeast of the array is close to the S75°E trend of the proposed transform faults in southern Iceland [*Ward*, 1971*a*]. Faults striking N10°E, S60°E, and N75°E were observed about 10 km to the

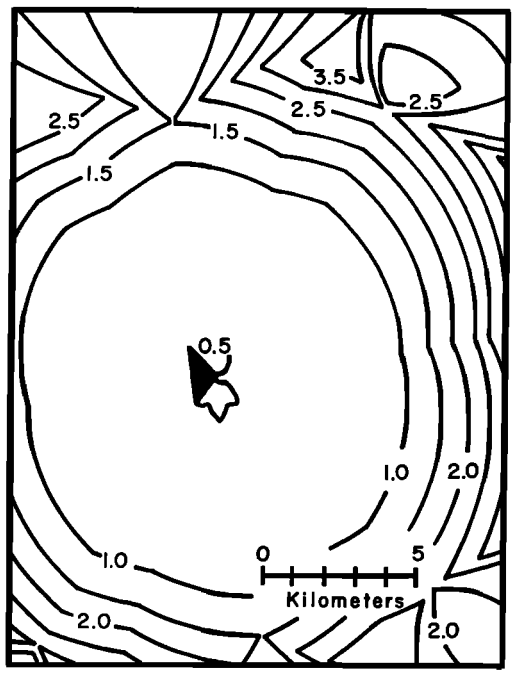


Fig. 9. Error in distance to epicenters located with data from the Hveragerdi array. The errors are plotted on the map shown in Figure 6. The numbers are the maximum distance minus the minimum distance in kilometers. The error is calculated assuming an error in reading the $P$ arrivals of $\pm 0.005$ sec and an error in reading the $S$–$P$ arrivals of $\pm 0.05$ sec. All earthquakes are assumed to occur at 3 km depth. The triangle is the array.

northeast [*Tryggvason*, 1955]. Faults trending S60°E were mapped just south of Hengill [*Saemundsson*, 1967; *Árnason et al.*, 1969].

Figure 11 shows all the events in Figure 6 projected onto a north-south cross section through the array. The larger ellipses represent earthquakes with the more clearly read phases. The zone of hypocenters appears to dip northerly 25° to 45°. Although any dip radial from the array could be explained by large errors in reading $S$–$P$ times, the probable errors are too small in this case, and the extent of this trend is too large for the dip to be considered fictitious.

*Locations of microearthquakes near Krísuvík.* Figure 12 shows 285 hypocentral locations based on data from the Krísuvík array in southwestern Iceland. The numbers denote depths to the nearest kilometer. The microearthquakes in this region are clustered in a much smaller volume than those events near Hveragerdi. There are two dominant features of the hypocentral distribution near Krísuvík: the very dense clustering of events under the southwestern edge of Kleifarvatn (Vatn means lake) and an east-northeast trending zone of activity southeast of the array. Hypocenters shown generally have calculated precisions (P. L. Ward, unpublished data, 1971) of about $\pm 2°$ in azimuth, better than $\pm 0.6$ km in distance, and $\pm 0.6$ km in depth. Figure 13 shows these same hypocenters projected onto an east-west vertical plane. The larger ellipses depict events with the most clearly distinguishable phases. A large percentage of events occur in a small volume under southwestern Kleifarvatn (Figures 12 and 13). The zone of earthquakes that trends nearly east, south of the array, plunges eastward at about 30°.

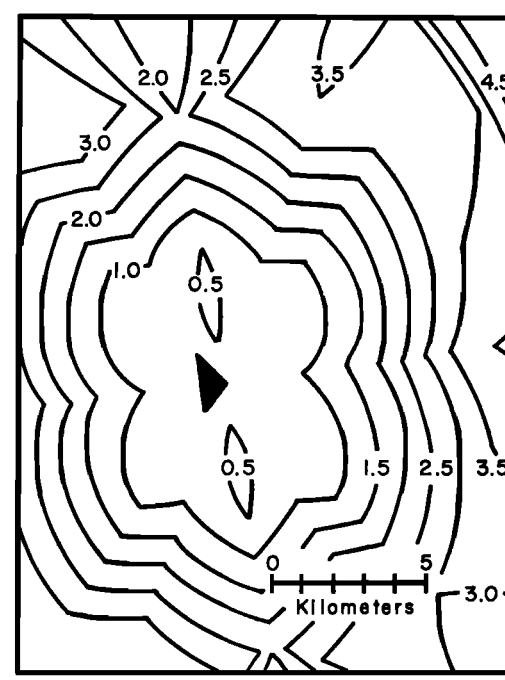


Fig. 10. Error in depth calculated for events near the Hveragerdi array. The errors are plotted on the map shown in Figure 6. The numbers are the maximum calculated depth minus the minimum calculated depth. All earthquakes are assumed to occur at 3 km depth. The errors are calculated assuming an error in reading the $P$ arrivals of $\pm 0.005$ sec and an error in reading the $S$–$P$ arrivals of $\pm 0.05$ sec.

Again the microearthquakes are confined to the region of geothermal activity defined by the outcrops of thermally altered rock. The major thermal activity generally occurs near the epicenters of the main microearthquake activity. Nevertheless, some fumaroles and mudpots, not associated with large numbers of microearthquakes, occur 1 km northeast of Graenavatn and 1 to 2 km northwest of Djúpavatn. Intense fumarolic activity occurs on the lake bottom above the main cluster of earthquakes. Analysis of $CO_2$ and $H_2$ fumarolic gas shows that the highest temperature in the Krísuvík area is in the range of 250°C.

*Locations of microearthquakes near Krafla.* Figure 14 shows the locations of 20 well-recorded earthquakes near the Krafla array in northern Iceland. The calculated azimuth of explosions in the volcanic crater Víti was 12° to the east of the true location (Table 7). This difference may be caused by lateral refraction along layers dipping westward and striking north-south parallel to many grabens, fissures, and lava flows in this area. At any rate, those events to the north of the array should be shifted westward by 12° in azimuth. There are no data on the accuracy of events to the south of the array. The precision in location of events near the array is about ±0.3 km in distance and depth. The three events to the southwest have a precision of ±1.5° in azimuth, ±0.5 km in distance, and ±1 km in depth. These events occur in a geothermal area having several producing wells on the west flank of Námafjall and several natural steam vents on the east flank. Krafla is a volcano that has not been active for at least 200 years [*Thórarinsson*, 1960]. A solfatara field and steam vents occur about 0.5 km south of Víti.

*Apparent decrease of activity away from the arrays.* There is an apparent decrease in earthquake activity away from the arrays in Figures 6, 12, and 14. The decrease in the number of events with distance from the array can be predicted by the following equation derived from *Asada* [1957] assuming that the events are uniformly distributed on a plane:

$$N = K \int_{x_1}^{x_2} x^{1-b} \exp(-bkx)\, dx \qquad (5)$$

where $N$ is the number of events at a hypocentral distance of from $x_1$ to $x_2$, and $K = \pi f/QV$. For $x$ less than the hypocentral depth, $N = 0$. The heavy line in Figure 15 represents $N$ for $Q = 150$, $f = 25$ cps, and velocity $V = 2.8 + 0.11x$. $N$ is shown as a function of S–P

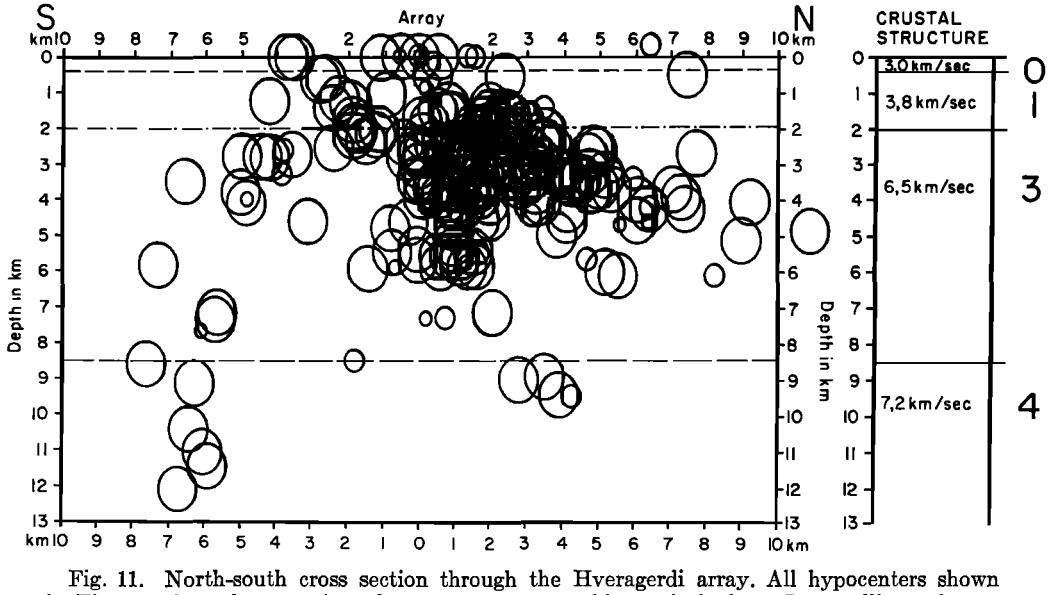


Fig. 11. North-south cross section through the Hveragerdi array. All hypocenters shown in Figure 6 have been projected east or west onto this vertical plane. Large ellipses denote earthquakes with more clearly read phases. The crustal structure was determined by *Pálmason* [1970].

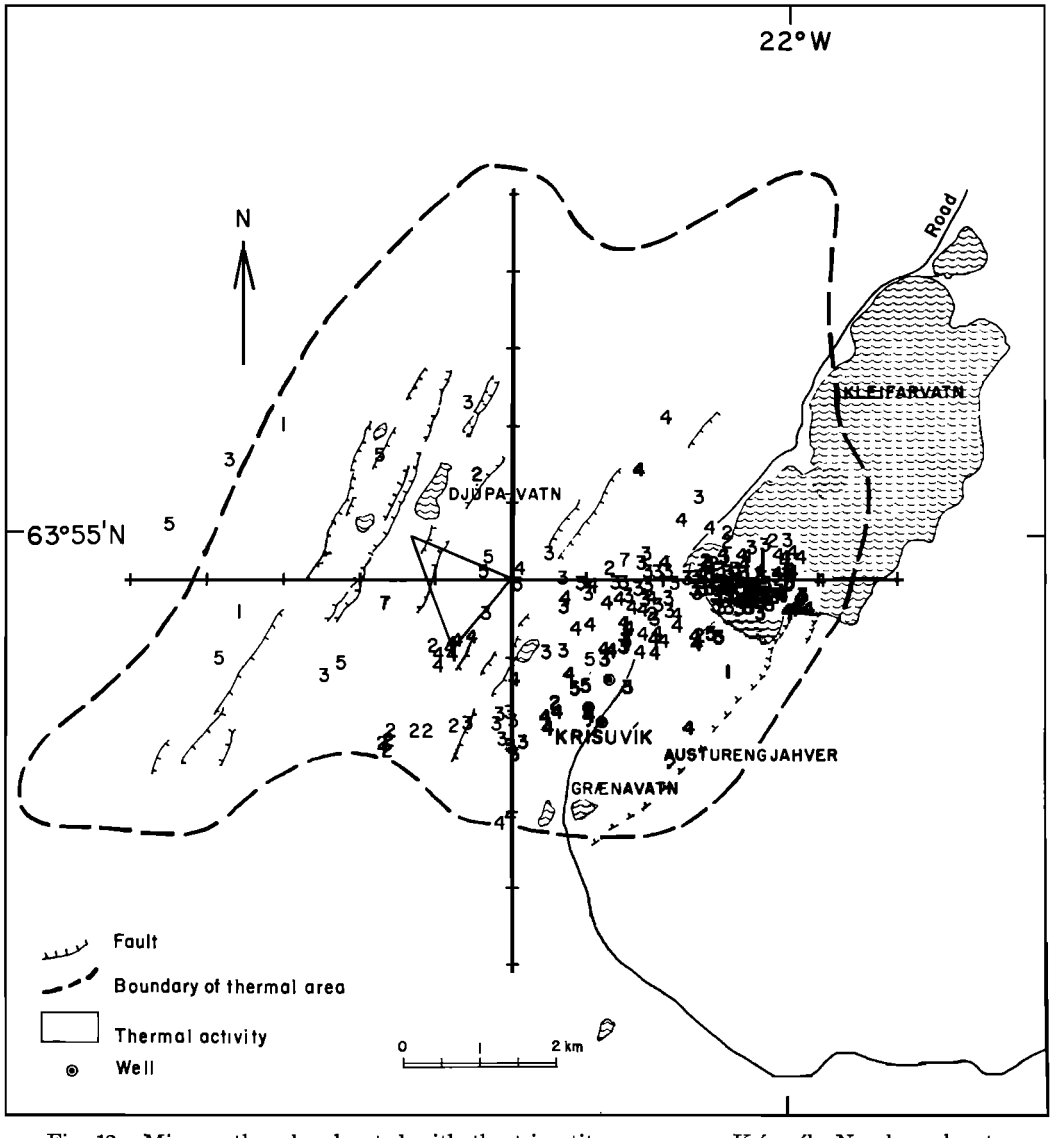


Fig. 12. Microearthquakes located with the tripartite array near Krísuvík. Numbers denote depths to the nearest km. The triangle is the array. Vatn means lake in Icelandic.

time ($T_{S-P}$) defined as

$$T_{S-P} = x(V_p - V_s)/V_s V_p \qquad (6)$$

The plane of earthquakes is assumed to be 3 km deep.

The dots in Figure 15 show the distribution of *S–P* times at Hveragerdi, and the triangles depict the distribution at Krísuvík. Clearly the microearthquakes are clustered at Krísuvík as seen in Figure 12. At Hveragerdi there is a clustering of events with *S–P* times between 0.4 and 0.7 sec, but otherwise the decrease of events toward the edges of the area shown in Figure 6 is nearly that predicted and, therefore, does not indicate a lower seismicity for *S–P* times $\leq$2.4 sec or distances $\leq$19 km. Thus, care must be taken in drawing any conclusions about the relative activity in one part of the area as opposed to another part simply on the basis of the number of mapped epicenters. On the other hand, the analysis in Figure 15 cannot distinguish relative activity as a function of

azimuth. Relative activity at the same distance but different azimuths can be directly compared. The area south of Hveragerdi, for example, has far lower activity than the area to the north, and there is a clear clustering of activity on the map.

*Depth of the earthquake activity and layer 3.* The most important result of this study of precise locations is that most of the well-located microearthquakes occurred between 2 and 6 km depth, a few less well located events being as deep as 13 km (Figures 11 and 13). These depths are the first well-determined depths of seismic activity in Iceland and, for that matter, along most of the mid-ocean ridge system.

Most of the hypocenters in Figures 11 and 13 occur near the top of layer 3, the crustal layer observed using seismic refraction methods to have a *P*-wave velocity of about 6.5 km/sec in Iceland [*Pálmason*, 1970] and about 6.7 km/sec elsewhere in the ocean [*Raitt*, 1963]. This layer is often referred to as the 'oceanic layer.' At Krafla, the depth of layer 3 changes from 3 km in the northern part of the map to 4 km in the southern part (Figure 14). Half the twenty foci are shallower than the top of layer 3. There are too few events here to be sure of their relationship to layer 3.

When detailed location of earthquakes is possible [e.g., *Eaton et al.*, 1970; *Hamilton et al.*, 1969], it is usually found that events at depths of less than 1 or 2 km are rare. It appears that stress sufficient for an earthquake with magnitude as low as −1 cannot generally accumulate at very shallow depths, at least in zones of existing fractures [*Scholz et al.*, 1969] and in zones of intense rifting such as those found in Iceland. Therefore, it might be argued that the spatial coincidence of microearthquakes with the upper part of layer 3 is simply fortuitous. The observation that layer 3 and the microearthquakes are both shallower in Hveragerdi than in Krísuvík, however, makes this relationship appear less accidental.

*Hess* [1959, 1965] thought that layer 3 in oceanic areas consists of serpentinite instead of basalt, as was commonly assumed at that time. *Cann* [1968] has proposed that layer 3 is basalt but metamorphosed to the amphibolite facies. *Pálmason* [1970] has suggested that the bound-

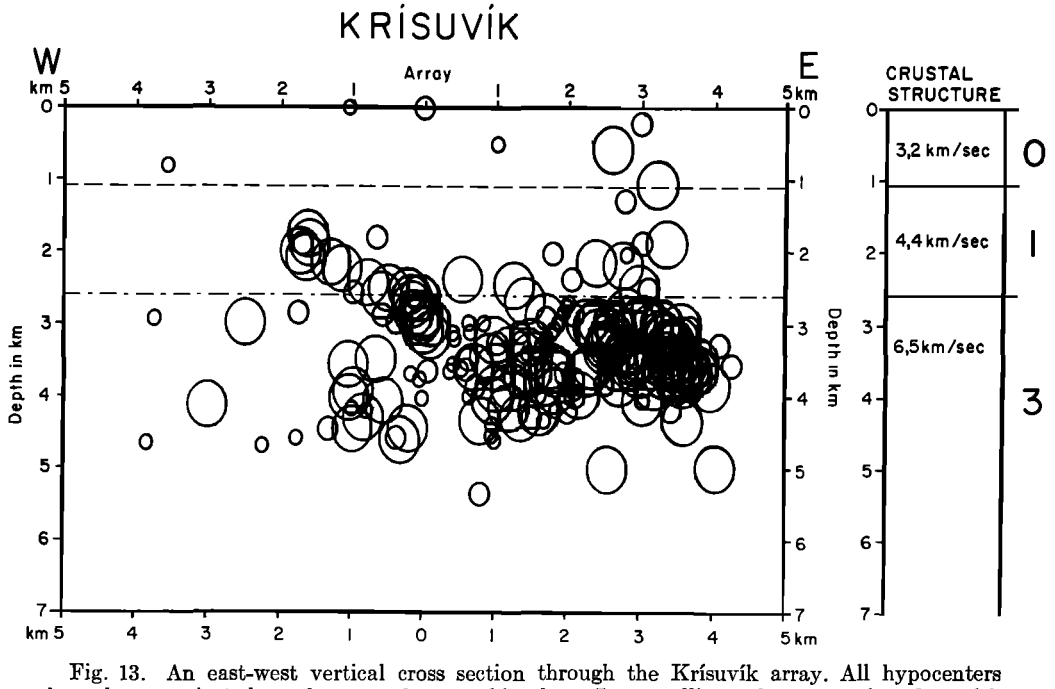


Fig. 13. An east-west vertical cross section through the Krísuvík array. All hypocenters have been projected north or south onto this plane. Larger ellipses denote earthquakes with more clearly read phases. The crustal structure was determined by *Pálmason* [1970].

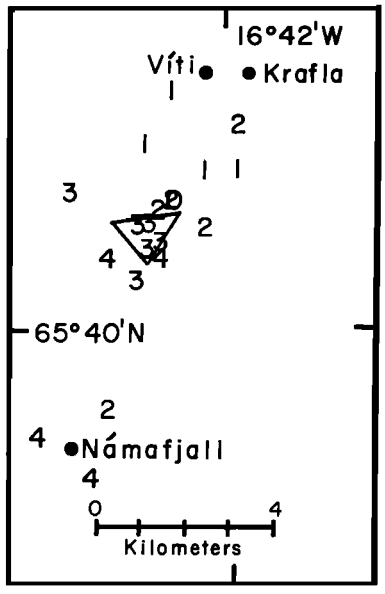


Fig. 14. Microearthquakes located with the tripartite array near Krafla. Numbers denote depths to the nearest kilometer. The triangle is the array.

ary between layers 2 and 3 in Iceland is a 350–400°C isotherm at the ridge crest and a paleoisotherm away from the ridge. He finds that layer 3 is quite shallow under central volcanoes and some geothermal areas. These observations imply that the boundary between layers 2 and 3 is some type of metamorphic front.

Combined gravity and seismic refraction data give an 8% increase in density between layer 2 and 3 [*Pálmason*, 1970]. The volume change associated with this increase might increase stresses near the boundary, particularly if the boundary is not planar.

Another possible explanation for the predominant occurrence of microearthquakes in layer 3 is that this layer is stronger than the layers above, and thus stress sufficient for seismic release can generally accumulate only in this layer or below. The deeply rifted layers above would be deformed aseismically. *Scholz et al.* [1969] presented a model for the San Andreas Fault that is similar in many aspects to this idea. Amphibolite has a higher ultimate strength than basalt in laboratory measurements [*Handin*, 1966]. The strength that is important when considering seismic release, however, is certainly more complex. One possibility is that, if layer 3 is a zone of active metamorphism, fractures may be quickly modified and welded so that large stress differences and stress drops are required for further slip or else new fractures must be formed.

## EARTHQUAKE SWARMS AND STRESS RELEASE IN GEOTHERMAL AREAS

In this paper, microearthquakes in Iceland were shown to occur in a number of small zones, most of which coincide spatially with geothermal areas. Large earthquakes apparently did not occur during the same time in the geothermal areas. Earthquakes have generally been felt near geothermal areas, but the data are generally insufficient to determine whether the epicenters are inside or outside these areas. The implication of the data in this paper, although it cannot yet be considered proven, is that microearthquakes occur reasonably continuously as swarms in the geothermal areas, but large earthquakes with their aftershock sequences are typical outside the geothermal areas.

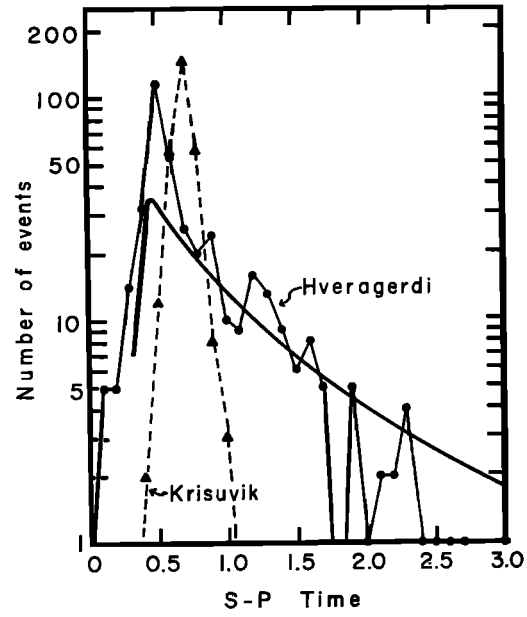


Fig. 15. The *S–P* time versus the number of earthquakes with a given *S–P* time for both the Hveragerdi and Krísuvík arrays. The curve shows the expected distribution of *S–P* times considering geometrical spreading and anelastic attenuation.

A swarm is a sequence of earthquakes that has no one outstanding principal event. The total seismic energy per unit time released in a swarm usually increases slowly to some peak and then decreases just as slowly or even more slowly. A main-shock sequence typically consists of a few or no foreshocks, one large mainshock, and many aftershocks. The seismic energy released in such a sequence usually increases almost as a step function and then decays nearly exponentially with time. Swarms have usually but not always occurred during volcanic eruptions and in regions of Cenozoic volcanic activity [e.g., *Richter,* 1958; *Eaton and Murata,* 1960; *Minakami,* 1960]. Geothermal areas around the world are also generally associated with Cenozoic volcanism. *Mogi* [1962, 1966] suggested from laboratory studies of rock fracturing that swarms are the characteristic mode of seismic energy release in nonuniform material, whereas aftershock sequences are characteristic of uniform material. *Sykes* [1970] observed swarms from mid-ocean ridge crests but not from fracture zones. *Thatcher and Brune* [1971] located a swarm on a ridge crest in the Gulf of California. In this paper, support is given for the hypothesis that swarms occur in regions where the crust is weakened yet strong enough to fracture so that some stress but not large stress can be sustained. The stress is therefore relieved in numerous small earthquakes. This crustal weakening might be attributed principally to the effects of fluid, fluid pressure, or chemical alteration. Several important considerations leading to this hypothesis will now be discussed in some detail.

*Large earthquakes near geothermal areas.* The only earthquakes reported by the U.S. Coast and Geodetic Survey for 1967, 1968, and 1969 in Iceland and located clearly very close to, if not in, a geothermal area were four events of magnitude 4.3 to 4.4 that occurred in September 1967 near the southwestern tip of the Reykjanes Peninsula. New ground fracturing in the thermal area was observed, and old and new hot springs erupted water up to 15 meters high. Sixteen strong events were felt at Reykjanes. The activity began on September 28 but reached its peak on September 30. The activity may have propagated from near Kleifarvatn to Reykjanes (R. Stefánsson, personal communication, 1968). This continuing activity with no single large event might best be considered as a swarm.

Only a few large earthquakes near geothermal areas have been well located. In August 1969, an event of magnitude 3.7 with aftershocks occurred about 5 km west-northwest of the Hengill geothermal area. This event was well located with the aid of portable seismographs. An event of magnitude 5.5 to 6.0 in December 1968 was located about 15 km east of Krísuvík. Local and teleseismic arrival times show that this event most likely occurred east of the Krísuvík geothermal area, but the data are not good enough to be sure that the earthquake did not occur in the small Brennisteinfjöll geothermal area, 5 km from the calculated epicenter.

The largest recorded earthquakes in southern Iceland (see summary by *Ward* [1970]), as well as the three events of magnitude 5, 4.7, and 4.6 in 1967, occurred along the one segment of the proposed fracture zone in southern Iceland where there are no known geothermal areas. One of the few zones of microearthquakes not associated with geothermal areas occurred in this same segment of the fracture zone. These microearthquakes were clearly foreshocks and aftershocks of the main shock, an event of magnitude 5, on July 27, 1967.

*Energy and numbers of microearthquakes.* It is well known that the energy released by an earthquake of magnitude 6 is about 1000 times greater than the energy of an event of magnitude 4 [*Gutenberg and Richter,* 1956], whereas only about 100 events of magnitude 4 can normally be expected to occur for each event of magnitude 6. Thus, it appears that the energy for a large earthquake is not likely to be relieved by a large number of small earthquakes.

Another variable that must be considered, however, is the volume of the earthquake activity. The geothermal areas constitute only a small part of the tectonically active zone in Iceland. The proposed transform fault zone in southern Iceland, for example, is about 150 km long between ridge crests [*Ward,* 1970]. There are six major geothermal areas in this fracture zone (Table 4, numbers 1–5 and 9) that extend along about 10% of its length. Thus, only about 10% of the stress in this fracture zone would need to be relieved by reasonably continuous swarm activity in the thermal areas, whereas about 90% could be relieved by large earth-

quakes. In addition, some of the stress could be relieved aseismically.

*Kisslinger* [1968] discussed the volumetric growth of the source region involved in the earthquake storm at Matsushiro, Japan. He concluded that the total energy density for the swarm approaches that expected for a single major earthquake with magnitude corresponding to the total energy release of the swarm. Furthermore, he pointed out that some of the largest earthquakes of the swarm occurred outside the central hypocentral zone of activity. He suggested that release of stress by the swarm in relatively weak rocks increases the stress on the stronger surrounding rocks to the point where they fracture.

*Sykes* [1970] found that swarms of teleseismically located earthquakes with magnitudes greater than 4 occur typically along ridge crests. In this study, however, microearthquake swarms have been confined to geothermal areas and appear to have occurred predominantly in the fracture zones. One way to reconcile these data is given by *Ward* [1970], who suggests that a number of short sections of ridge crest occur within the transform fault zone in southern Iceland and that many of the geothermal areas appear to occur at the junction of ridge crests with the individual transform faults. The microearthquake swarms might, therefore, be related to the segments of ridge crest and might then only be expected to account for a very minor fraction of the total stress relieved by earthquakes. The first motions of microearthquakes at Krísuvík, however, generally suggest strike-slip motion rather than the dip-slip motion expected from earthquakes along ridge crests. More detailed first motion data are needed before a firm conclusion can be reached. More data are also required to calculate the amount of energy or the seismic slip dissipated in different parts of the assumed fracture zone.

*Fluid pressure.* One possible explanation for the microearthquake activity in the geothermal areas is that water, particularly water under pressure, weakens the crust in these regions. The role of water in triggering earthquakes has been emphasized, for example, at the Rocky Mountain Arsenal fluid injection well in Denver, Colorado [*Evans*, 1966], at the Rangely oil field in Colorado [*Raleigh et al.*, 1970], and for the Matsushiro earthquake swarm in Japan [*Nakamura*, 1969]. The Denver earthquake sequence could certainly be considered a swarm, since the seismic activity increased slowly to a peak over five years [*Healy et al.*, 1968].

During the summer of 1968, a tripartite array was operated near Hveragerdi, as described above, specifically to see whether operation of a large geothermal well near station *A* of the array would significantly affect the microearthquake activity. This well (well 8) is 300 meters deep and has a natural flow of 130 kg/sec of water and steam. The number of earthquakes per hour with *S–P* times of less than 1.5 sec are shown in the bar graph in Figure 16. Periods when the well was open are denoted by the broad horizontal bars along the time axis. Only events with amplitudes greater than 18 mm were counted because some events of smaller amplitude could have been missed. Although there was little microearthquake activity when the well was open on July 20, August 4, and August 10, periods when the well was opened for 6 to 7 days show no substantial difference in activity from other times. There is an apparent decrease in activity after the first opening of the well, but this change appears to be fortuitous, since it was not reproduced during later openings of the well. Examination of the spatial distribution of these microearthquakes shows no difference in the locations of events occurring when the well was opened or closed. Thus, operation of the well does not appear to affect significantly the occurrence of microearthquakes.

One reason that the operation of the well does not seem to influence the microearthquake activity could be that the earthquakes are generally deeper than 2 km, whereas the well is only 0.3 km deep. Furthermore, the fluid pressure at the base of the well is observed to decrease about 12% owing to heating of the fluid in the well hole when the well was flowing. In the Rocky Mountain Arsenal well in Denver, Colorado, the average monthly fluid pressure at the base of the well was increased by as much as 54% of the initial fluid pressure [*Healy et al.*, 1968].

It is not clear that high fluid pressures are likely to exist in the geothermal areas in Iceland. High pressures at the well head are generally due to superheated water flashing to steam in the well pipe. The artesian pressures at the top of a closed-in well are usually less

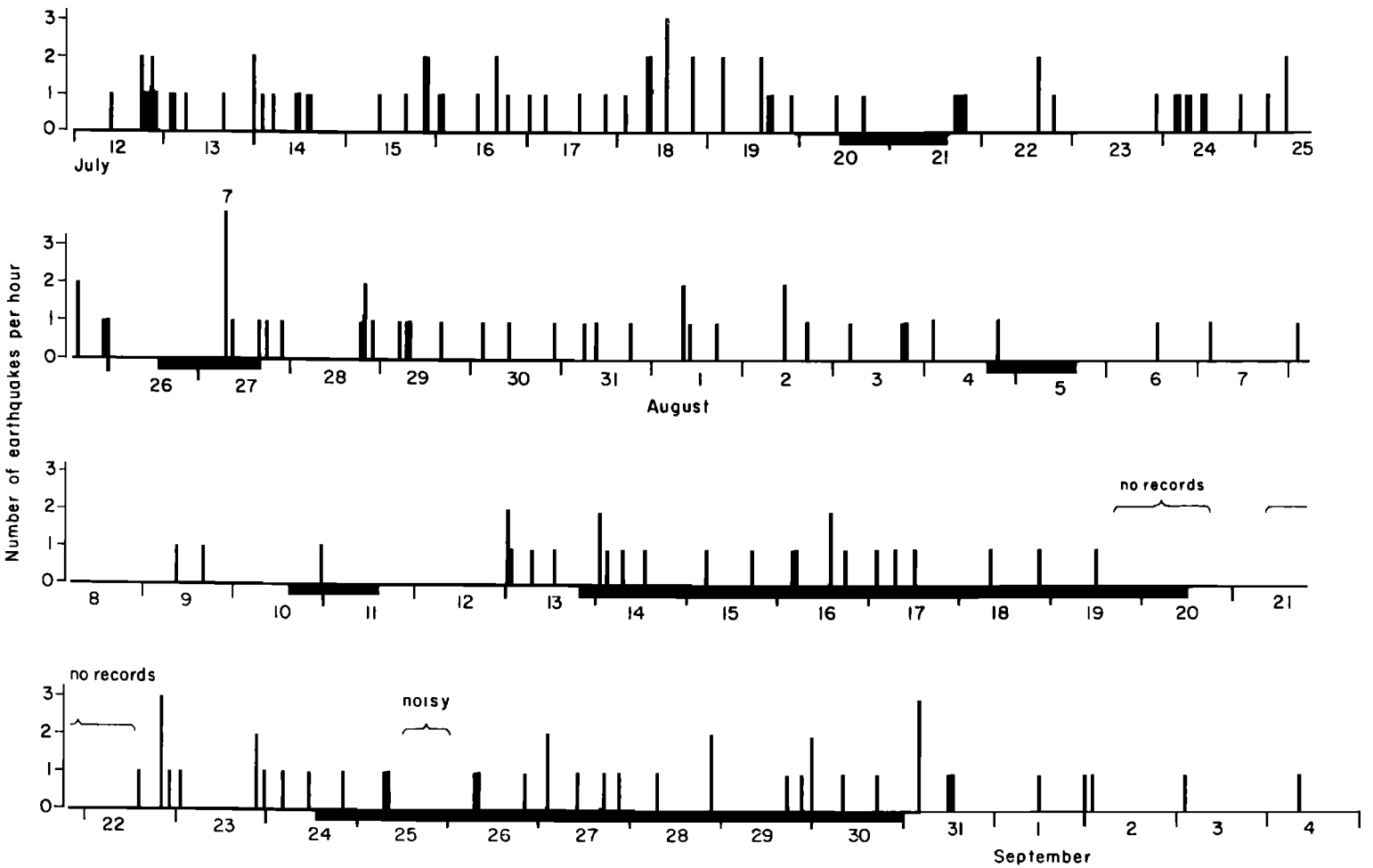


Fig. 16. A histogram of events per hour recorded at the Hveragerdi array. Broad horizontal bars depict periods when geothermal well 8 was discharging.

than a few bars. In order to get high fluid pressures at a given depth, some impermeable zone must exist that allows the fluid pressure to increase above the normal hydrostatic pressure. Such barriers may not form in active fracture zones.

Very high fluid pressures may not be needed, however, for triggering earthquakes. The regional least principal stress in Iceland seems to be horizontal, since Iceland is near the crest of the mid-Atlantic ridge and thrust faulting is not observed. In zones of rifting where normal faulting predominates, the least stress may be very small. It has been proposed that earthquakes are triggered when the pore pressure is simply sufficient to reduce the normal force across a fracture below some critical level [*Hubbert and Rubey*, 1959; *Healy et al.*, 1968]. In a transform fault zone, the deviatoric normal stress across individual fractures will vary slightly, depending on whether the fracture lies along the trend of the over-all fault zone or lies several degrees from it. In some regions within a fracture zone, there may be strike-slip faults with large components of thrust or normal faulting. Thus, the amount of fluid pressure needed to trigger earthquakes may vary greatly along a given fault zone.

The hydrostatic pressure in the thermal areas is lower than in surrounding regions. For example, at 3 km depth the temperature is about 180°C outside the thermal area in Iceland [*Pálmason*, 1967*a*] and about 360°C with a thermal area where the water is boiling at every depth. The corresponding hydrostatic pressures would be 260 and 200 bars, respectively. The lithostatic pressure might be about 745 bars in both regions.

In the thermal areas with boiling water at every depth, the viscosity of the water at a depth of 3 km is about 0.4 millipoise and the density is about 0.3, whereas outside the thermal areas the viscosity is about 2.3 millipoise and the density is 0.9 [*Dorsey*, 1968]. Thus high-temperature fluids are far more penetrating. Perhaps the viscosity of the fluid should be included in models for the effects of fluid pressure. At the Rocky Mountain Arsenal well in Denver, for example, the natural temperature at the base of the well may be about 100 to 140°C. If water is pumped down at 25°C, it would have a viscosity of about 8.9 millipoise. When pumping stops, the water would eventually heat up to 120°C and the viscosity would fall to about 2.3 millipoise. The continuation of the earthquake activity after pumping stopped could, therefore, be partly explained by better penetration of the pore fluid because of a decrease in viscosity.

*Water and earthquake swarms.* It has long been known that water substantially weakens rocks under compression in the laboratory. One reason is the effect of pore pressure described above. Another reason is stress corrosion [*Scholz*, 1968], where the water produces corrosion reactions that take place preferentially at points of high tensile stress. Although stress corrosion does not appear to be important at room temperature [*Brace and Martin*, 1968], it is exponentially dependent on temperature and thus may well be of far greater importance in geothermal regions and at typical hypocentral depths. Stress corrosion need not only be thought of in terms of microscopic cracks. Fluids circulating along a fault, for example, leach out silica, etc., from irregularities in the fault surface. This leaching weakens the irregularities and could thus decrease the coefficent of static friction, allowing slip to occur.

Water in a geothermal area probably circulates to depths of many kilometers. A geothermal aquifer was found near the bottom of a borehole 2.2 km deep in Iceland [*Pálmason*, 1967*a*]. Pálmason argues that the proper conditions may exist in the zone of active rifting and volcanism for free convection of water to at least this depth. *Banwell* [1963] tentatively suggested that water in the Wairakei geothermal area in New Zealand might circulate to depths of several kilometers. Thus, it does not seem unreasonable to expect that surface water circulates to the depths of many if not most of the microearthquakes located in this paper.

The data in this paper, through not conclusive, are consistent with the hypothesis that water in geothermal areas leads in some way to a weakening of the crustal rocks. The rocks then deform in response to regional stresses, and earthquake activity in these weakened areas tends to be dominated by swarms of small events. The swarms are frequent and sometimes long lived. The stronger crust outside the weakened areas fractures less often, but larger

stresses are accumulated and these stresses are relieved in mainshock-aftershock sequences.

## CONCLUSIONS

In this paper, microearthquake data are presented from a reconnaissance survey in which portable seismometers were used throughout most of Iceland and from a detailed survey with tripartite arrays in three geothermal areas in Iceland. The most important conclusions from the work are as follows:

1. Most of the microearthquakes recorded in Iceland occurred in 13 zones that were generally less than 5 km in radius. The number of events recorded near the zones averaged from 0.4 to 23 events per day. At most recording sites throughout the country, few or no microearthquakes were recorded.

2. The numbers of events per day based on short periods of recording are only generally representative of the over-all activity at each site. Large variations may occur rarely. The chance of recording a daily count that is within $\pm 45\%$ of the daily mean based on two months of recording, in the example given, increased from 60% after one day of recording to 65% after two days and 70% after three days.

3. The number of microearthquakes recorded in a particular zone in 1968 generally, but not always, was within 30% of the number recorded there in 1967.

4. Few data would have been recorded in this study if portable instruments had not been within 30 km of the active zones. This fact emphasizes the importance or placing high-gain, portable seismometers at many sites throughout the region to be studied.

5. Nine of the thirteen zones of microearthquakes in Iceland coincide spatially with geothermal areas. Two other zones are in areas of submarine volcanism where geothermal areas may occur. One microearthquake zone is near an acidic intrusion and one is an aftershock zone.

6. Geothermal areas that are structurally related to fissure systems generally have microearthquake activity, whereas those areas that have few prominent fissures and seem only to be related to acidic intrusions have little or no microearthquake activity.

7. The locations of the zones of microearthquakes across southern Iceland support the hypothesis of a transform fault near 64°N trending west-northwest.

8. Large differences were noted between observed and expected azimuths and apparent velocities for earthquakes and explosions at many azimuths and distances greater than 18 km from the Hveragerdi array. Most of these differences can be explained by an interface dipping 2° to 5° between two crustal layers, but other explanations are possible. These observations demonstrate the necessity for using explosions or independently located earthquakes to find the accuracy of hypocenters determined with data from a tripartite array.

9. Most of the well-located microearthquakes in Iceland occurred at depths of 2 to 6 km in the uppermost part of crustal layer 3. Some events were as deep as 13 km.

10. Epicenters of microearthquakes in two areas where detailed location was possible were confined primarily to the zone of thermal alteration observed at the surface. The greatest earthquake activity was often near the regions of greatest thermal activity observed at the surface.

11. Operation of a geothermal well did not significantly affect the occurrence of microearthquakes nearby.

12. It is suggested that stress along the fractures zone in southern Iceland is relieved by numerous swarms of microearthquakes in the geothermal areas but by mainshock-aftershock sequences elsewhere along the transform fault between the two ridge crests. Aseismic creep may be present in either region. The crust in the geothermal areas may well be weakened by the physical or chemical effects of water or by fluid pressure. According to this model, the probability of recording microearthquakes in the geothermal areas in Iceland is substantially higher than the probability of recording some microearthquakes outside the geothermal areas, but in the fracture zone. This difference in probability results simply from the fact that swarms are more continuous in time than aftershock sequences.

*Acknowledgments.* C. L. Drake, P. Einarsson, J. Kelleher, A. Kjerulf, S. Magnússon, and L. Sykes assisted in the field work. T. Sigurgeirsson of the University Science Institute, Reykjavik, provided a tape recorder and other equipment,

as well as laboratory space and encouragement. G. Pálmason of the National Energy Authority assisted with the logistics, encouraged us during the project, and generously provided an advance look at his refraction data before publication. J. Oliver, L. R. Sykes, B. Isacks, and S. Ward contributed significantly in reviewing the manuscript, and C. Scholz provided some comments. We deeply appreciate all this assistance.

This research was supported by National Science Foundation grant GA-1534. Some details of this study were completed with the aid of grant 8 from the Arthur L. Day Fund of the National Academy of Sciences. Some equipment was obtained on NSF grant GP 4815 awarded to the Science Institute, University of Iceland.

## REFERENCES

Árnason, B., P. Theodórsson, S. Björnsson, and K. Saemundson, Hengill, a high temperature thermal area in Iceland, *Bull. Volcanol., 33,* 245, 1969.

Arnórsson, S., A geochemical study of selected elements in thermal waters of Iceland, Ph.D. thesis, University of London, 353 pp., 1969.

Arnósson, S., J. Jónsson, and J. Tómasson, General aspects of thermal activity in Iceland, *23rd Int. Geol. Congr., 18,* 77, 1969.

Asada, T., Observations of nearby microearthquakes with ultrasensitive seismometers, *J. Phys. Earth, 5,* 83, 1957.

Banwell, C. J., Thermal energy from the earth's crust, Introduction and Part 1, *N.Z. J. Geol. Geophys., 6,* 52, 1963.

Berninghausen, W. H., A checklist of Icelandic volcanic activity, *Bull. Seismol. Soc. Amer., 54,* 443, 1964.

Björnsson, S., Hot springs and thermal energy, *Iceland Rev., 5*(2), 35, 1967.

Bödvarsson, G., Physical characteristics of natural heat sources in Iceland, *Jökull, 11,* 29, 1961.

Brace, W. F., and R. J. Marton, III, A test of the law of effective stress for crystalline rocks of low porosity, *Int. J. Rock Mech. Min. Sci., 5,* 415, 1968.

Brune, J., and C. R. Allen, A microearthquake survey of the San Andreas fault system in Southern California, *Bull. Seismol. Soc. Amer., 57,* 277, 1967.

Cann, J. R., Geological processes at mid-ocean ridge crests, *Geophys. J., 15,* 331, 1968.

Dorsey, N. E., *Properties of Ordinary Water Substance,* p. 43, Hafner Publ. Co., New York, 1968.

Eaton, J. P., and K. J. Murata, How volcanoes grow, *Science, 132,* 925, 1960.

Eaton, J. P., M. E. O'Neill, and J. N. Murdock, Aftershocks of the 1966 Parkfield-Cholame, California, earthquake, *Bull. Seismol. Soc. Amer., 60,* 1151, 1970.

Evans, D. M., Man-made earthquakes in Denver, *Geotimes, 10,* 11, 1966.

Ewing, J., and M. Ewing, Seismic-refraction measurements in the Atlantic Ocean basins, in the Mediterranean Sea, on the mid-Atlantic ridge, and in the Norwegian Sea, *Bull. Geol. Soc. Amer., 70,* 291, 1959.

Friedman, J. D., R. S. Williams, Jr., G. Pálmason, and C. D. Miller, Infra-red surveys in Iceland: Preliminary report, *U.S. Geol. Survey Prof. Paper, 650-C,* 89, 1969.

Gutenberg, B., *Physics of the Earth's Interior,* Academic, New York, 190 pp., 1959.

Gutenberg, B., and C. L. Richter, Magnitude and energy of earthquakes, *Ann. Geofis., 9,* 1, 1956.

Hamilton, R. M., F. A. McKeown, and J. H. Healy, Seismic activity and faulting associated with a large underground nuclear explosion, *Science, 166,* 601, 1969.

Handin, J., Strength and ductility, *Geol. Soc. Amer. Mem. 97,* 223, 1966.

Healy, J. H., W. W. Rubey, D. T. Griggs, and C. B. Raleigh, The Denver earthquakes, *Science, 161,* 1301, 1968.

Hess, H. H., The AMSOC hole to the earth's mantle, *Trans. AGU, 40,* 340, 1959.

Hess, H. H., Mid-oceanic ridges and tectonics of the sea floor, in *Submarine Geology and Geophysics,* 1965 Colston Symposium, edited by W. F. Whittard and R. Bradshaw, *Colston Papers, 17,* 317, 1965.

Hubbert, M. K., and W. W. Rubey, Role of fluid pressure in mechanics of overthrust faulting, 1, Mechanics of fluid-filled porous solids and its application to overthrust faulting, *Bull. Geol. Soc. Amer., 70,* 115, 1959.

Ishimoto, M., and K. Iida, Observations sur les Seismes Enregentre par le microseismograph construit dermerement, *Bull. Earthquake Res. Inst., 17,* 443, 1939.

Kisslinger, C., Energy density and the development of the source region of the Matsushiro earthquake swarm, *Bull. Earthquake Res. Inst., 46,* 1207, 1968.

Lange, A. L., and W. H. Westphal, Microearthquakes near the Geysers, Sonoma County, California, *J. Geophys. Res., 74,* 4377, 1969.

Matumoto, T., and P. L. Ward, Microearthquake study of Mt. Katmai and vicinity, Alaska, *J. Geophys. Res., 72,* 2557, 1967.

Minakami, T., Fundamental research for predicting volcanic eruptions, *Bull. Earthquake Res. Inst., 38,* 497, 1960.

Mogi, K., Study of elastic shocks caused by the fracture of heterogeneous materials and its relations to earthquake phenomena, *Bull. Earthquake Res. Inst., 40,* 125, 1962.

Mogi, K., Earthquakes and fractures, *Tectonophysics, 5,* 35, 1966.

Nakamura, K., Surface faulting during the Matsushiro earthquakes, *Trans. AGU, 50,* 389, 1969.

Niazi, M., Corrections to apparent azimuths and travel time gradients for a dipping Mohorovicic discontinuity, *Bull. Seismol. Soc. Amer., 56,* 491, 1966.

Norrman, J. O., Kustomorfologiska studier på Surtsey, *Svensk Naturvetenskap, 5,* 60, 1969.

Oliver, J., A. Ryall, J. N. Brune, and D. B. Slemmons, Microearthquake activity recorded by portable seismographs of high sensitivity, *Bull. Seismol. Soc. Amer., 56,* 899, 1966.

Pálmason, G., Seismic refraction investigation of the basalt lavas in northern and eastern Iceland, *Jokull, 13,* 40, 1963.

Pálmason, G., On heat flow in Iceland in relation to the mid-Atlantic ridge, in *Iceland and Mid-Ocean Ridges,* edited by S. Björnsson, *Soc. Sci. Islandica Publ. 38,* 111, 1967*a*.

Pálmason, G., Upper crustal structure in Iceland, in *Iceland and Mid-Ocean Ridges,* edited by S. Björnsson, *Soc. Sci. Islandica Publ. 38,* 67, 1967*b*.

Pálmason, G., Crustal structure of Iceland from explosion seismology, Science Institute, University of Iceland, (mimeographed doctoral thesis), 1970. (Also in *Soc. Sci. Islandica, 40,* 188 pp., 1971).

Raitt, R. W., The crustal rocks, in *The Sea,* edited by M. N. Hill, p. 85, Interscience, New York, 1963.

Raleigh, C. B., J. Bohn, and J. H. Healy, Earthquakes and fluid pressures in the Rangely oil field, Colorado, *Trans. AGU, 51,* 351, 1970.

Richter, C. F., *Elementary Seismology,* p. 71, W. F. Freeman and Co., San Francisco, 1958.

Romney, C., Amplitudes of seismic body waves from underground nuclear explosions, *J. Geophys. Res., 64,* 1489, 1959.

Saemundsson, K., Vulkanismus und tektonik des Hengill-Gebietes in Südwest-Island, *Acta Naturalia Islandica, 2*(7), 105 pp., 1967.

Scholz, C. H., Mechanism of creep in brittle rock, *J. Geophys. Res., 73,* 3295, 1968.

Scholz, C. H., M. Wyss, and S. W. Smith, Seismic and aseismic slip on the San Andreas fault, *J. Geophys. Res., 74,* 2049, 1969.

Seeber, L., M. Barazangi, and A. Nowroozi, Microearthquake seismicity and tectonics of coastal northern California, *Bull. Seismol. Soc. Amer., 60,* 1669, 1970.

Stauder, W., and A. Ryall, Spatial distribution and source mechanism of microearthquakes in central Nevada, *Bull. Seismol. Soc. Amer., 57,* 1317, 1967.

Stefánsson, R., Some problems of seismological studies on the mid-Atlantic ridge, in *Iceland and Mid-Ocean Ridges,* edited by S. Björnsson, *Soc. Sci. Islandica Publ. 38,* 80, 1967.

Sykes, O. R., Earthquake swarms and sea-floor spreading, *J. Geophys. Res., 75,* 6598, 1970.

Thatcher, W., and J. N. Brune, Seismic study of an oceanic ridge earthquake swarm in the Gulf of California, *J. Geophys. Res.,* in press, 1971.

Thórarinsson, S., The postglacial history of the Mývatn area and the area between Mývatn and Jökulsá á Fjöllum, in *On the Geology and Geophysics of Iceland, Guide to Excursion A2, Int. Geol. Congr. Norden, 21st,* 60, 1960.

Thórarinsson, S., *Surtsey, The New Island in the North Atlantic,* 47 pp., Viking Press, New York, 1967.

Tobin, D. G., P. L. Ward, and C. L. Drake, Microearthquakes in the Rift Valley of Kenya, *Geol. Soc. Amer. Bull., 80,* 2043, 1969.

Tryggvason, E., Surface deformation on and near three volcanoes in Iceland, *Trans. AGU, 51,* 441, 1970.

Tryggvason, T., On the stratigraphy of the Sog Valley in NW Iceland, *Acta Natur. Island. 1*(10), 35, 1955.

Ward, P. L., A new interpretation of the geology of Iceland: A detailed study of the boundary between lithospheric plates, Part 1, Ph.A. thesis, Columbia University, 159 pp., 1970.

Ward, P. L., and K. H. Jacob, Microearthquakes in the Ahuachapan geothermal field, El Salvador, Central America, *Science,* in press, 1971.

Ward, P. L., G. Pálmason, and C. Drake, Microearthquake survey and the mid-Atlantic ridge in Iceland, *J. Geophys. Res., 74,* 665, 1969.

(Received October 20, 1970;
revised February 9, 1971.)